IMT Atlantique
Bretagne-Pays de la Loire
École Mines-Télécom

COLLEGES SCIENCES
BRETAGNE POUR L'INGENIEUR
LOIRE ET LE NUMERIQUE

NON-COHERENT DETECTION OF CONTINUOUS PHASE MODULATION FOR LOW EARTH ORBIT SATELLITE IOT COMMUNICATIONS AFFECTED BY DOPPLER SHIFT

ANOUAR JERBI

Supervised by:

Frédéric GUILLOUD (IMT Atlantique)
Karine AMIS (IMT Atlantique)
Tarik BENADDI (Thales Alenia Space)

In collaboration with :

TéSA

Funded by :

Brest Métropole

ThalesAlenia Space

14/03/2023

The Internet of Things (IoT)

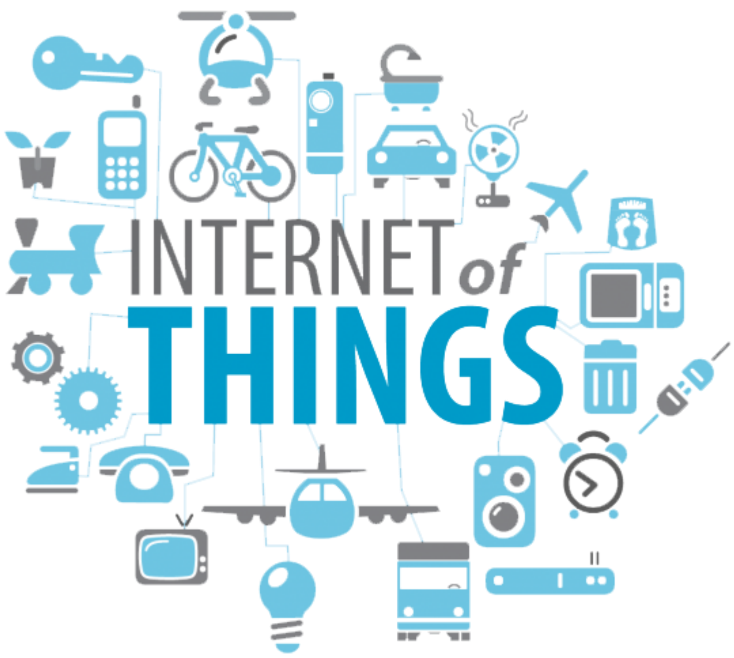

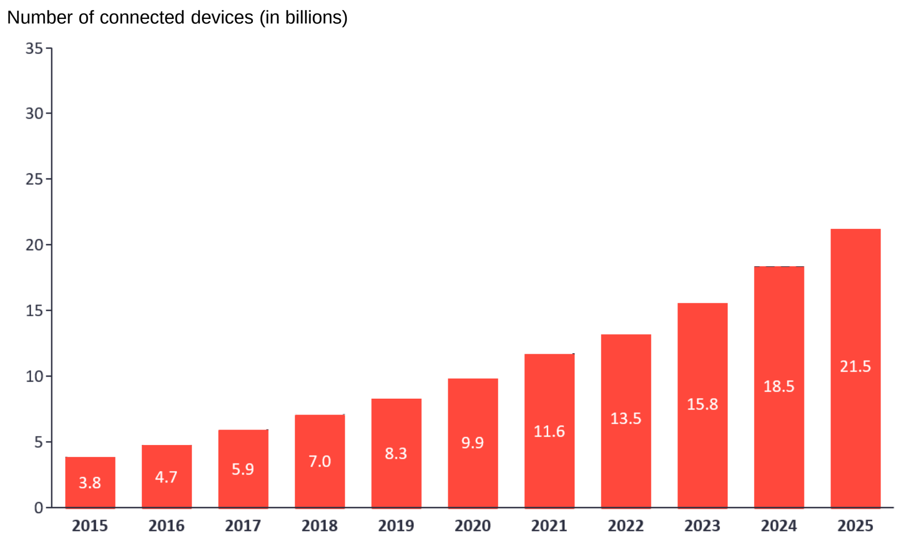

Figure : The number of connected devices in previous years and the expected number in 2024 and 2025

- The market is expected to grow by 19% in 2023 !

Source : IoT Analytics (www.iot-analytics.com)

IoT architecture

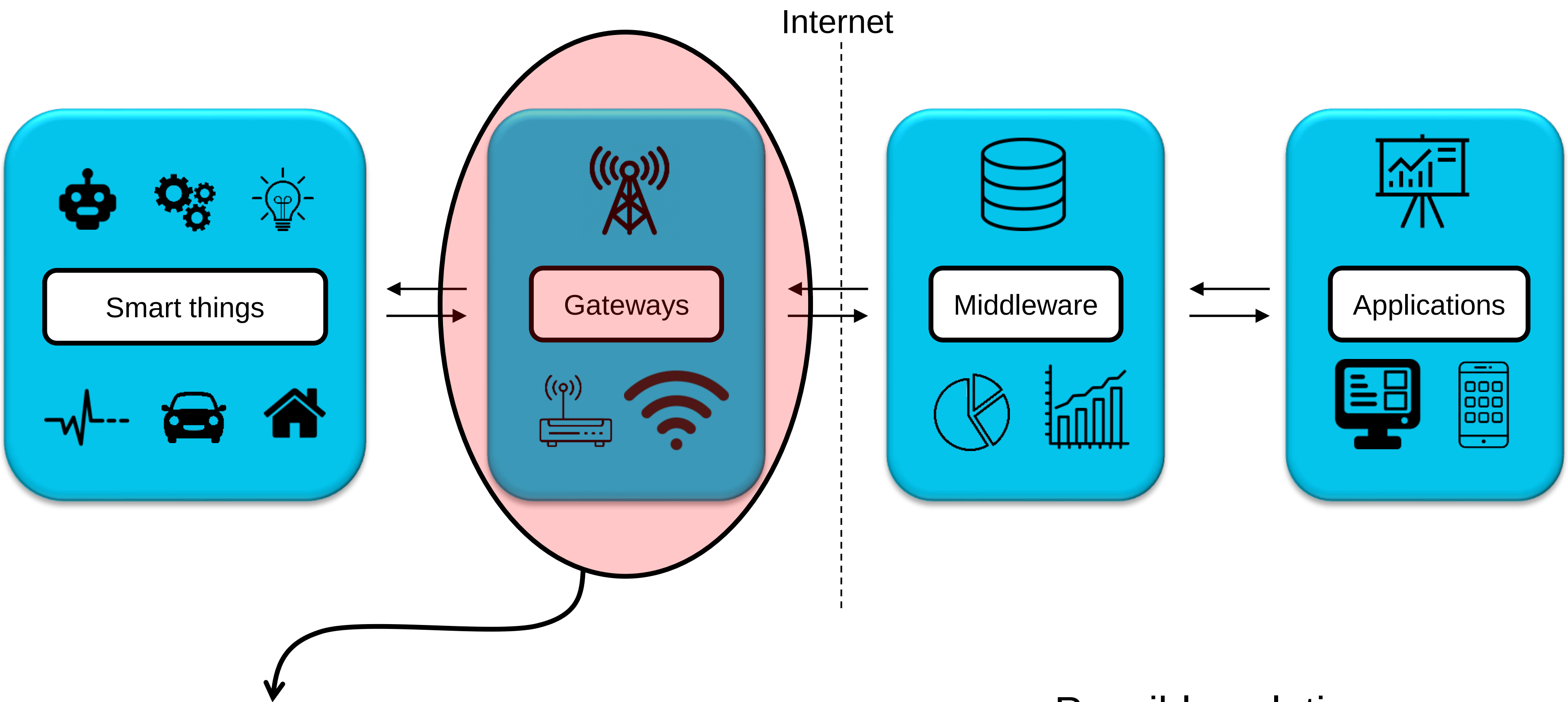

⚠ Not always simple to install ! ➡ Possible solution :

✓ Use satellites

Satellite usage with IoT

Best choice :
✓ LEO satellites

→ offers the best link budget for this application

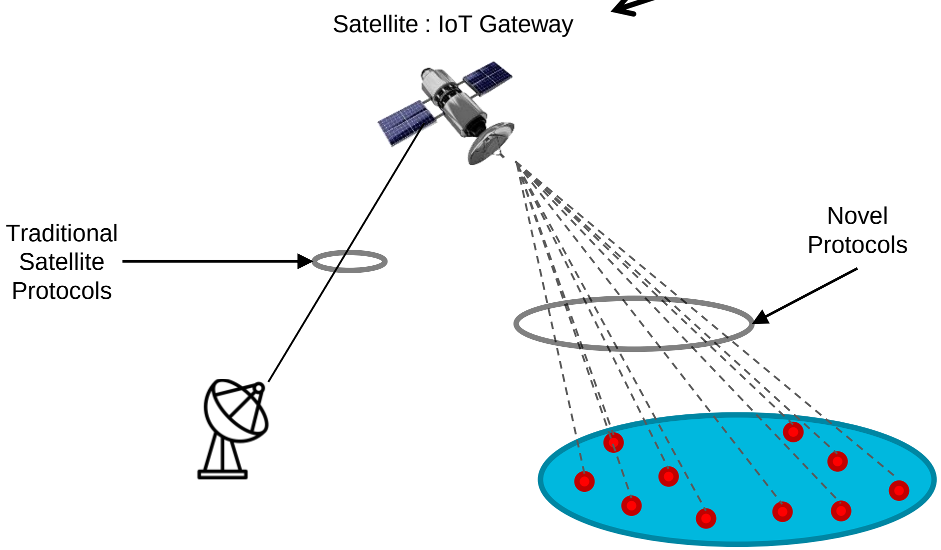

Must use new adapted communication techniques !

Direct-to-Satellite IoT

- ✓ Seamless worldwide coverage
- ✓ No need for terrestrial infrastructure

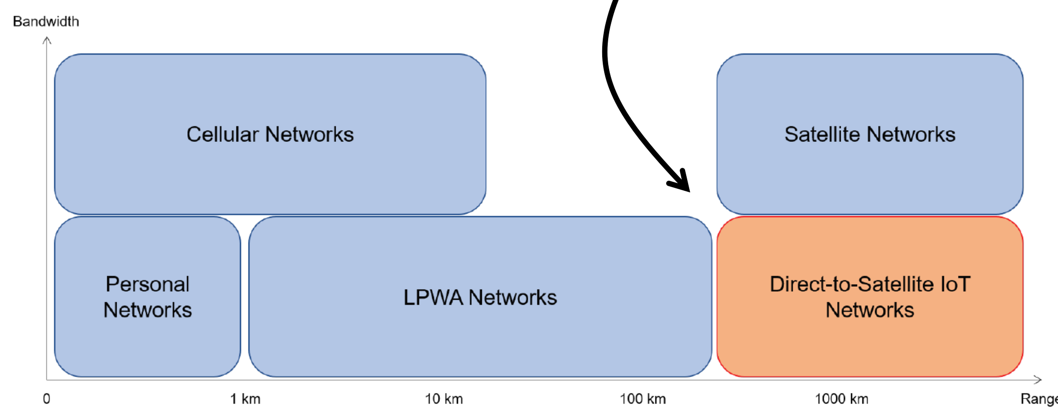

Figure : Bandwidth versus range for different types of networks

Satellite usage with IoT

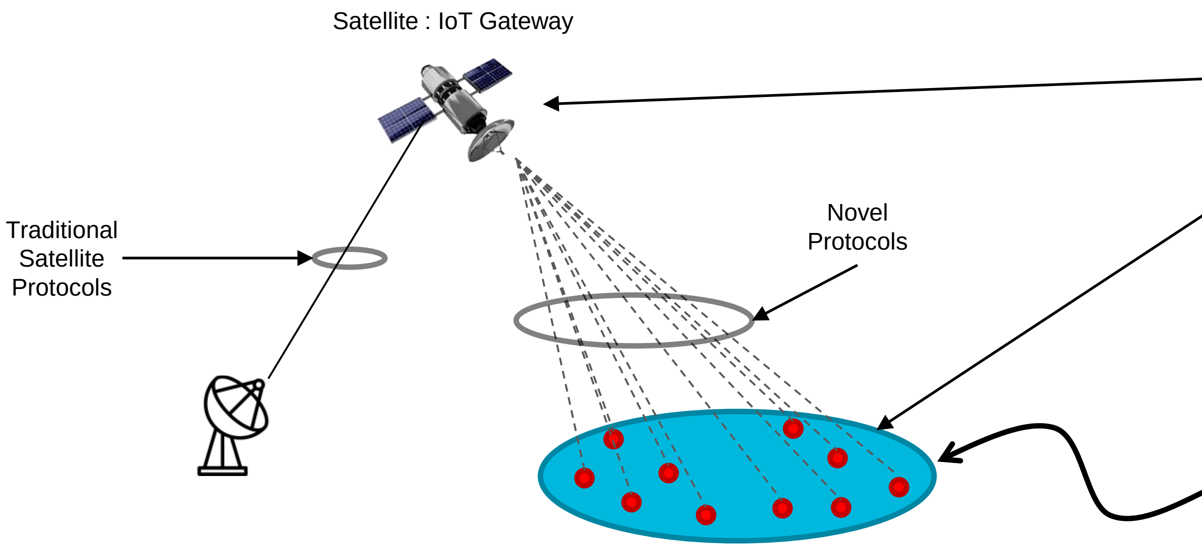

Non linear amplifiers used onboard the satellite and in the objects!

→ use constant envelope modulation

Huge number of communicating devices using free bands !

→ need for good spectral properties

→ Possible solution :

- ✓ Continuous Phase Modulation (CPM)

The Doppler problem

- LEO satellites travel at very high velocity.
- It can reach around 7.5 km/s.

⚠ Heavy **Doppler** present in the object-satellite link !

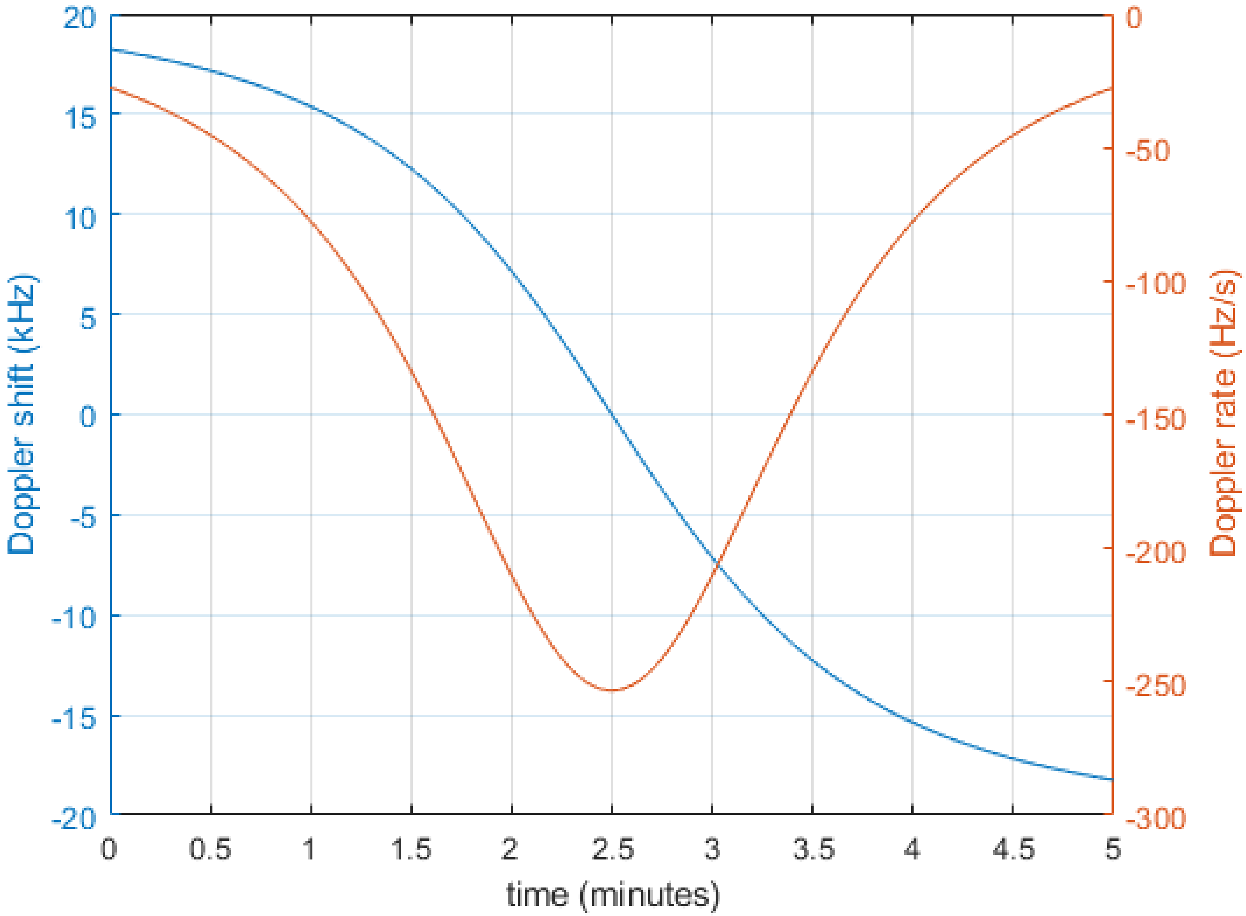

Figure : Typical Doppler shift and rate profiles received from a LEO satellite with 868 MHz carrier at an altitude of 550 km

CONTENT

IMT Atlantique
Bretagne-Pays de la Loire
École Mines-Télécom

CPM

IMT Atlantique
Bretagne-Pays de la Loire
École Mines-Télécom

Signal model

Continuous Phase Modulation (CPM) :

$$s(t, \mathbf{a}) = \sqrt{\frac{2E_s}{T_s}} \mathrm{e}^{j\theta(t,\mathbf{a})}$$

$$\theta(t, \mathbf{a}) = 2\pi h \sum_{i=0}^{N-1} a_i q(t - iT_s)$$

$$q(t) = \begin{cases} \int_0^t g(u)du, & 0 \leq t < LT_s \\ \frac{1}{2}, & \forall t \geq LT_s \end{cases}$$

a : modulation alphabet of order M

h : modulation index

g : frequency pulse shape

L : CPM memory

(a) $L = 1$

(b) $L = 5$

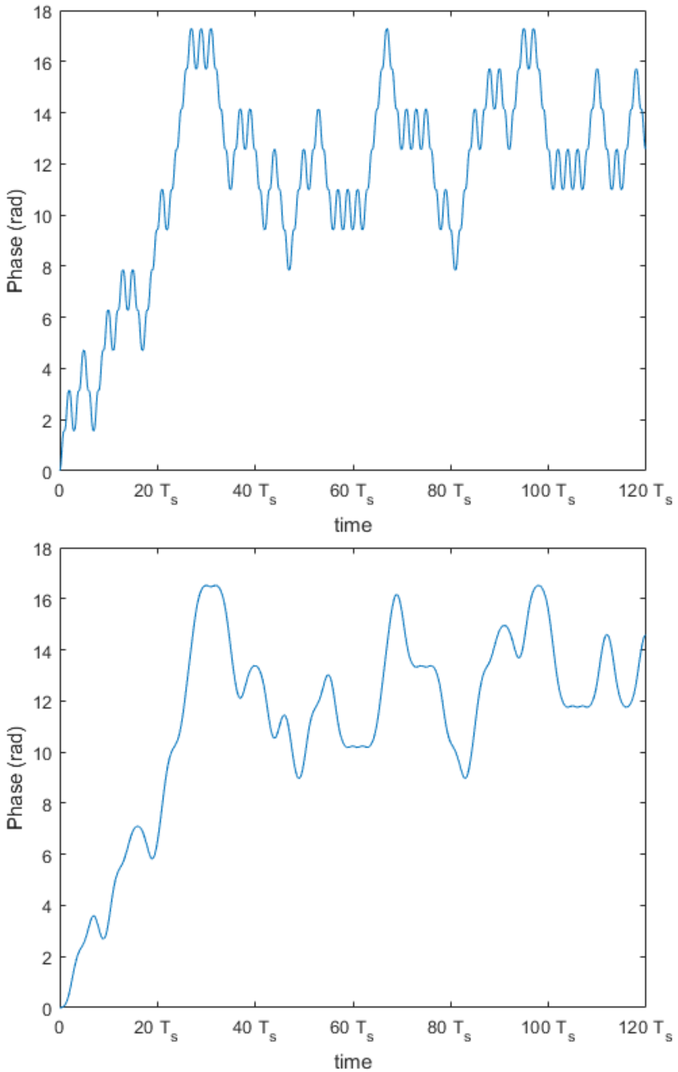

Figure : Phase evolution with time for binary RC, $h = 0.5$

Linear decomposition

Laurent decomposition of CPM [1] (extended by Morelli & Mengali [2]) :

$$s(t,\mathbf{a}) = \sqrt{\frac{2E_s}{T_s}} \sum_{k=0}^{K_T-1} \sum_{i=0}^{N-1} \alpha_{k,i} h_k(t - iT_s)$$

$$\boldsymbol{\alpha}_i = \{\alpha_{k,i}\}_{0 \le k \le K_T} = f(a_i)$$

$\boldsymbol{\alpha}_0$	$\boldsymbol{\alpha}_1$	$\boldsymbol{\alpha}_2$	$\boldsymbol{\alpha}_3$	$\boldsymbol{\alpha}_4$	
$\alpha_{0,0}$	$\alpha_{0,1}$	$\alpha_{0,2}$	$\alpha_{0,3}$	$\alpha_{0,4}$	..
$\alpha_{1,0}$	$\alpha_{1,1}$	$\alpha_{1,2}$	$\alpha_{1,3}$		
$\alpha_{2,0}$	$\alpha_{2,1}$	$\alpha_{2,2}$			
$\alpha_{3,0}$	$\alpha_{3,1}$				
$\alpha_{4,0}$					
⋮					

$$P = \log_2(M)$$

Components	Duration
first component	$L+1$
next $2^P - 2$ components	L
next $(2^P - 1)^2$ components	$L-1$
next $2^P(2^P - 1)^2$ components	$L-2$
next $2^{2P}(2^P - 1)^2$ components	$L-3$
.	.
.	.
last $2^{(L-2)P}(2^P - 1)^2$ components	1

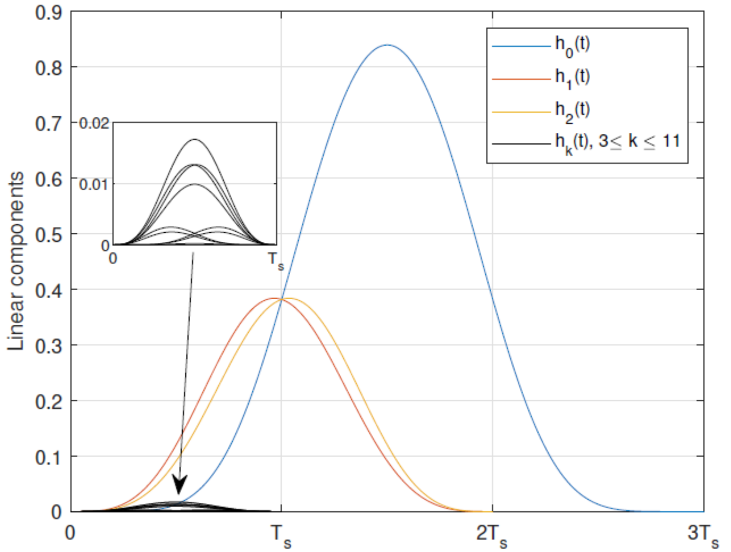

Figure : Linear components of the <u>Quaternary 2RC with *h* = 0.25</u>

[1] P. Laurent, “Exact and approximate construction of digital phase modulations by superposition of amplitude modulated pulses (AMP),” IEEE Trans. on Commun., vol. 34, no. 2, pp. 150–160, 1986.
[2] U. Mengali and M. Morelli, “Decomposition of M-ary CPM signals into PAM waveforms,” IEEE Trans. on Inf. Theory, vol. 41, no. 5, pp. 1265–1275, 1995.

Linear decomposition

Approximation to K_p principle components :

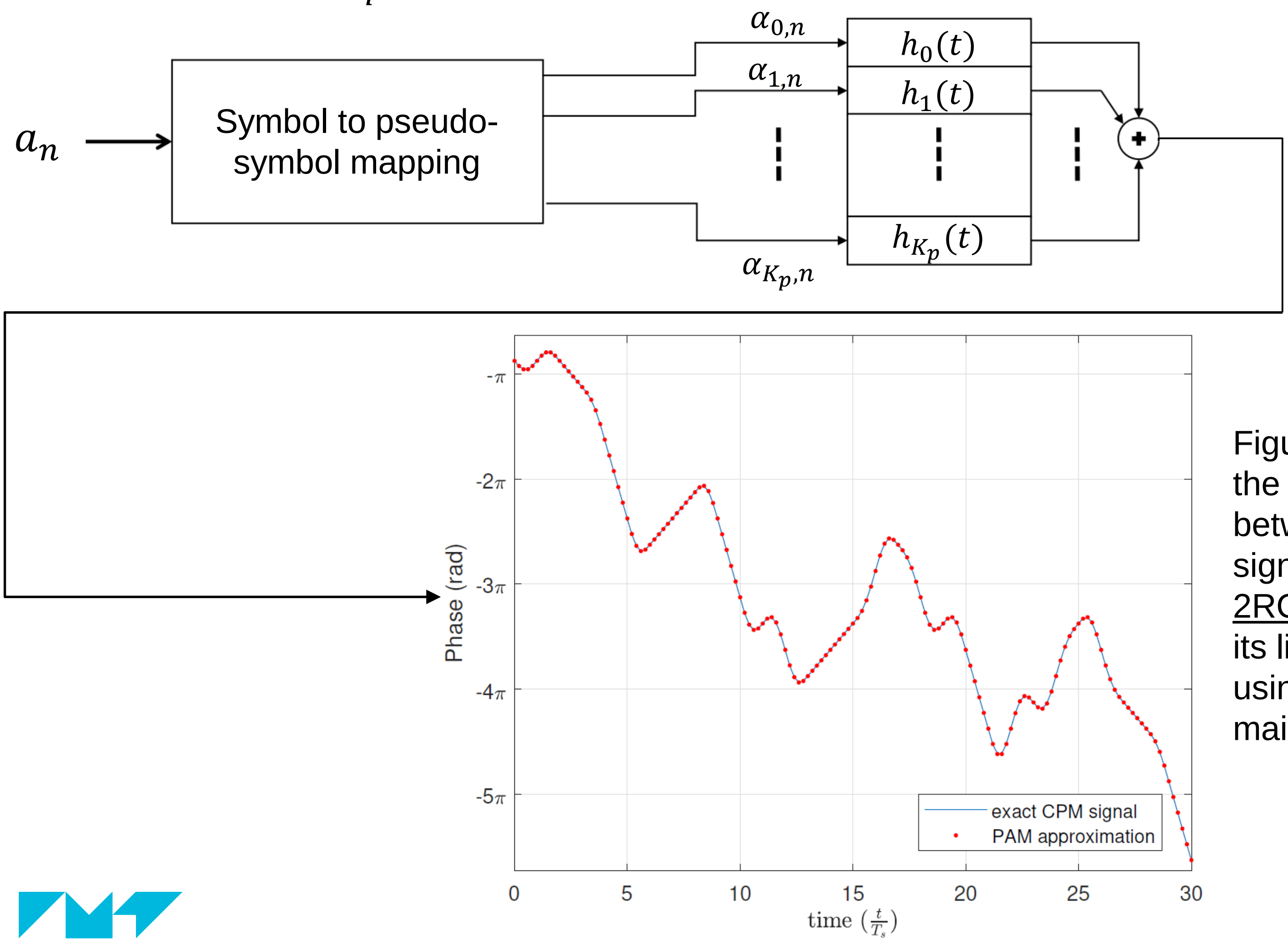

Figure : Comparison of the signal phase between the exact signal of the Quaternary 2RC with h = 0.25 and its linear approximation using only the first 3 main components

Coherent detection in AWGN

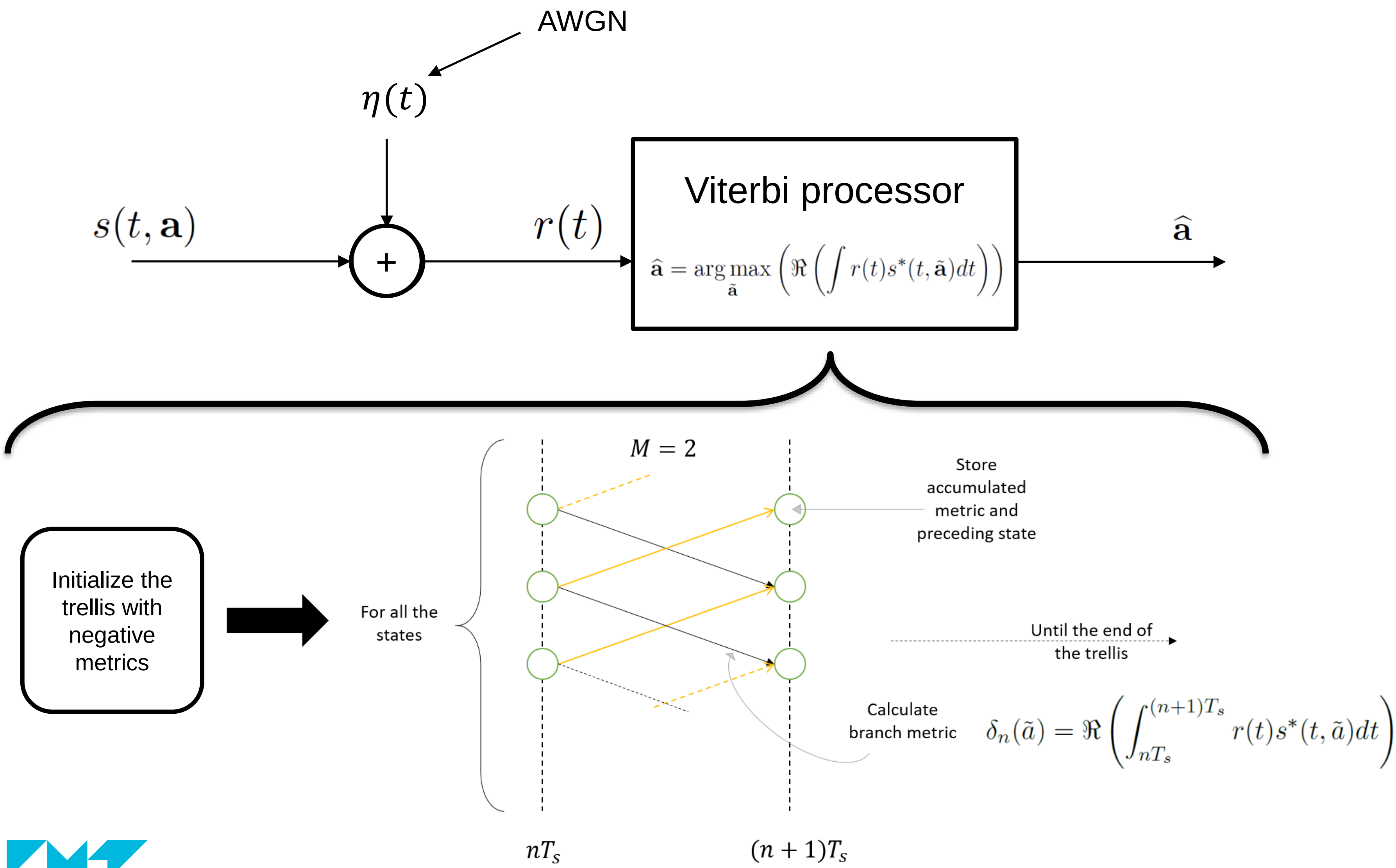

Coherent detection issues

- Problems with coherent detection in this application :
  - ⚠ Highly sensitive to phase mismatch
  - ⚠ Highly sensitive to Doppler estimation errors
  - ⚠ Need to use pilot symbols

➢ Use non coherent detection approach !
  - ✓ Act on the detection criterion
  - ✓ Act on the received signal

State of the art on Non coherent Sequence Detection (NSD)

Transmission model :

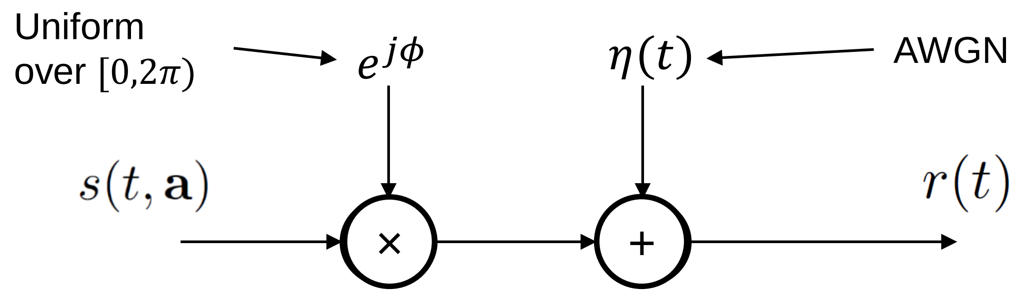

The receiver [1]:

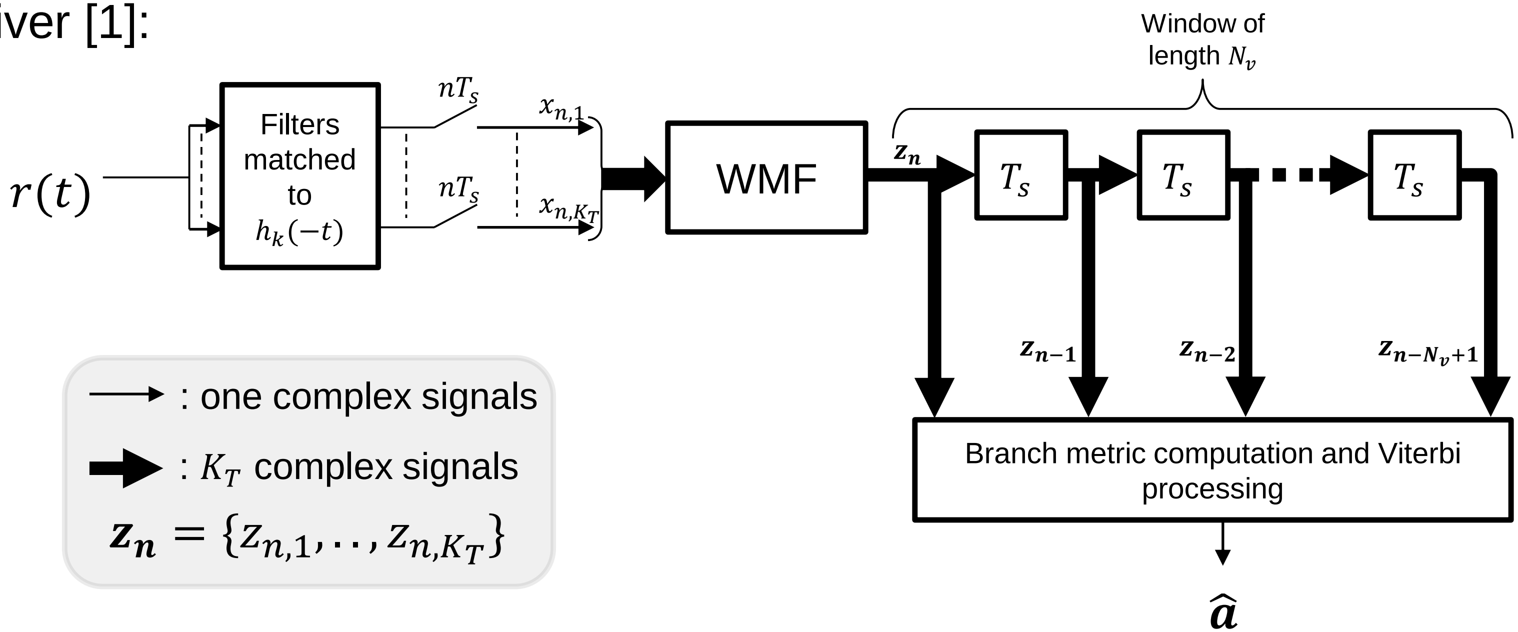

[1] G. Colavolpe and R. Raheli, "Noncoherent Sequence Detection of Continuous Phase Modulations," IEEE Transactions on Communications, vol. 47, no. 9, pp. 1303–1307, 1999.

Performance of NSD receiver

- Influence of the size of the detection window :

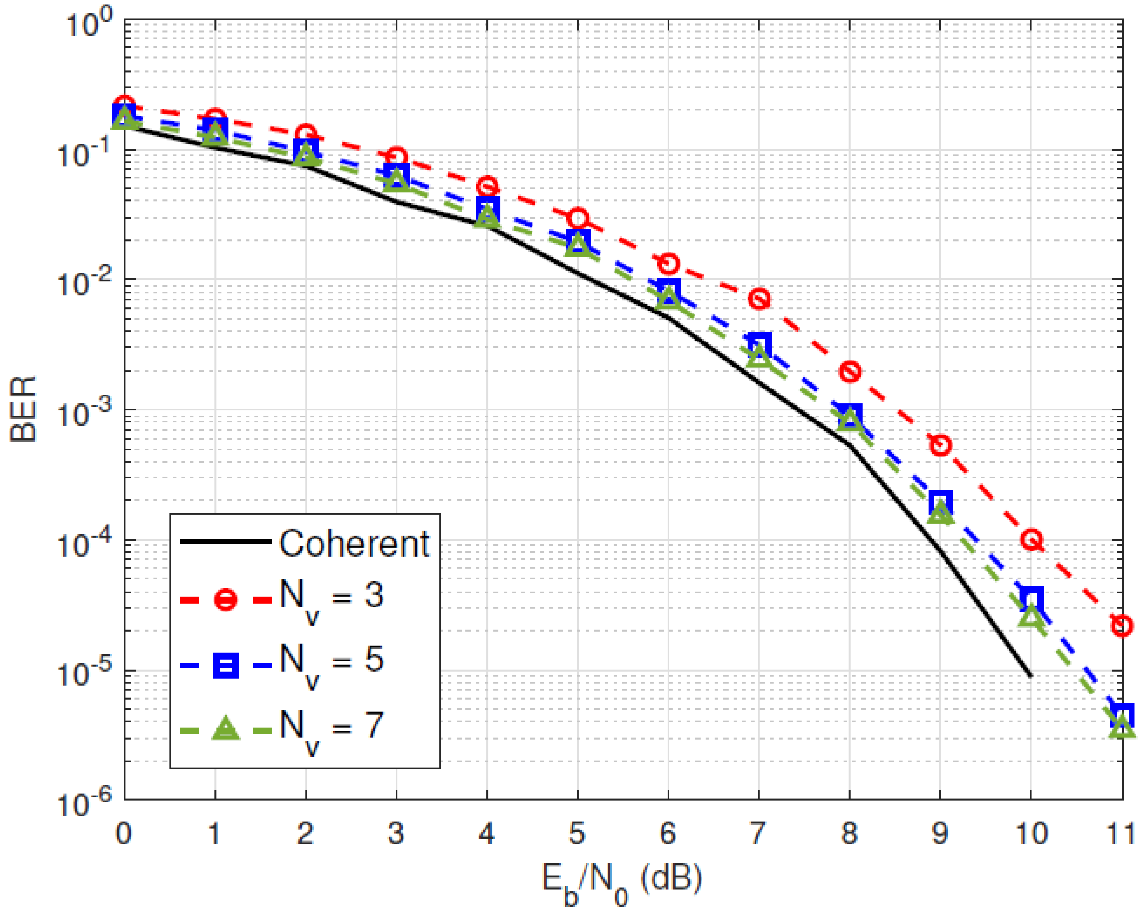

Figure : Performance of NSD receiver for the GMSK for different values of the estimation window compared to coherent detector on an AWGN channel

NSD receiver issues

- Problem with NSD receiver in the Satellite IoT:
  - ⚠ Need to use pilot symbols to estimate the Doppler
  - ⚠ Pilot sequence length might be high
- This is a limitation in short frame IoT communications !

➢ Need to use a blind approach

State of the art on differential detection

Transmission model :

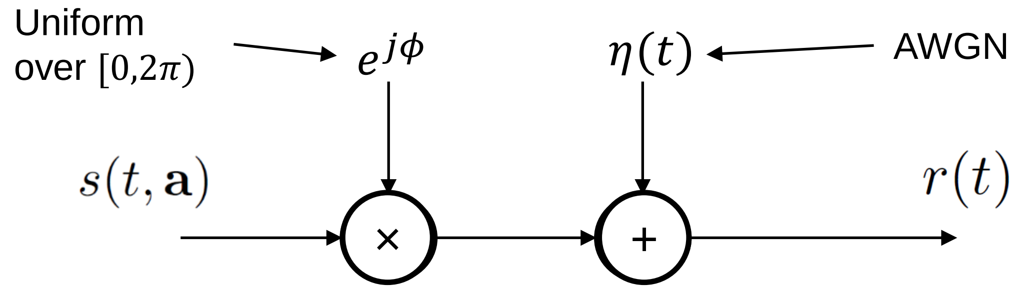

The receiver [1]:

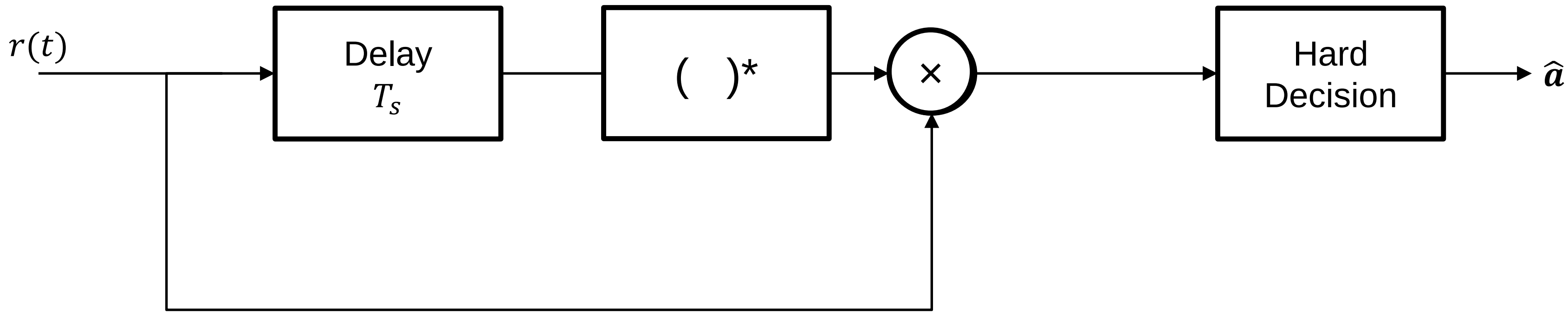

[1] M. Simon and C. Wang, “Differential Versus Limiter - Discriminator Detection of Narrow-Band FM,” IEEE Transactions on Communications, vol. 31, no. 11, pp. 1227–1234, 1983..

Performance of the differential receiver

→ significant performance degradation compared to coherent detection !

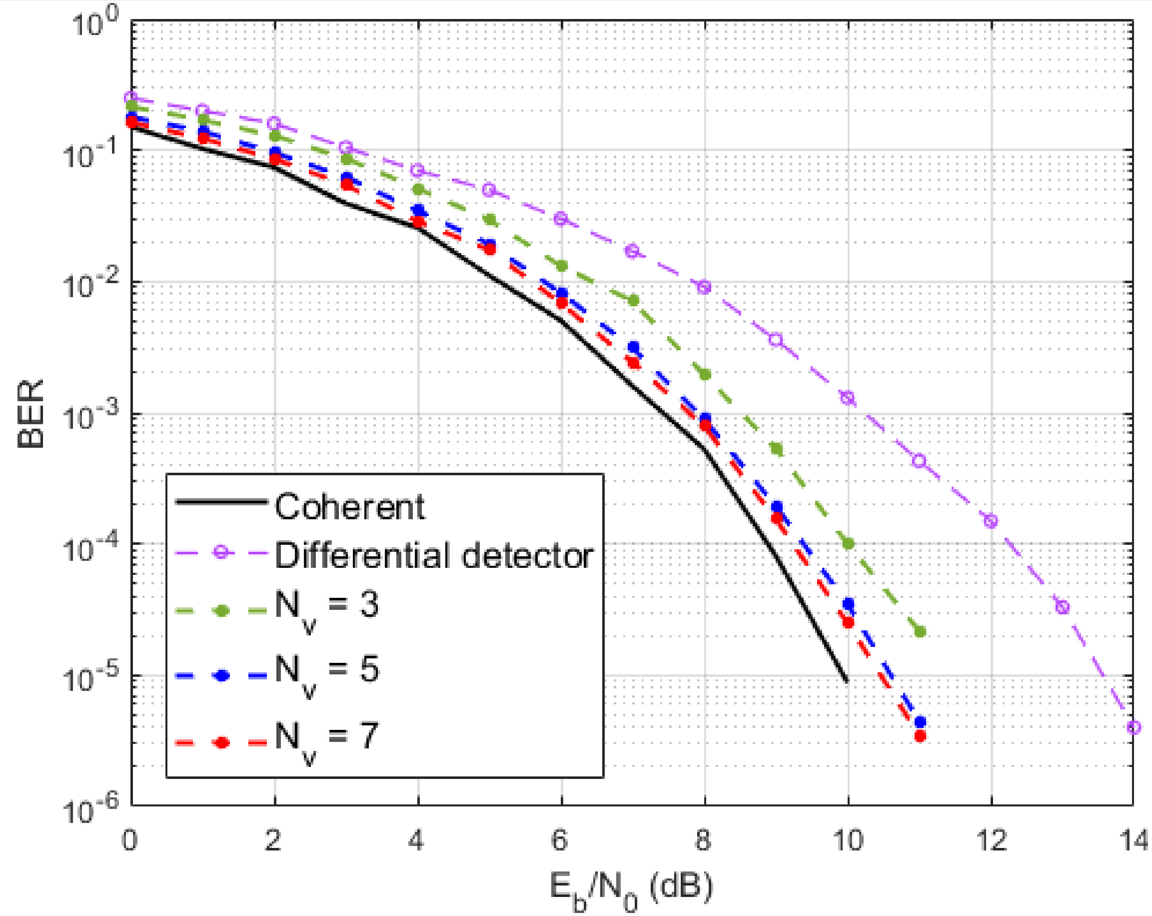

Figure : Performance of the differential receiver from [1] for GMSK on a AWGN channel

[1] M. Simon and C. Wang, "Differential Versus Limiter - Discriminator Detection of Narrow-Band FM," IEEE Transactions on Communications, vol. 31, no. 11, pp. 1227–1234, 1983.

The differential approach

- Differential detection for the Satellite IoT :
  - ✓ Easy to implement

⚠ Does not offer the best performance results !

- Need a solution to enhance performance
  - ➢ Use multiple symbols differential approach

CPM DETECTION WITH BLIND DOPPLER ESTIMATION

IMT Atlantique
Bretagne-Pays de la Loire
École Mines-Télécom

The new non coherent detection approach

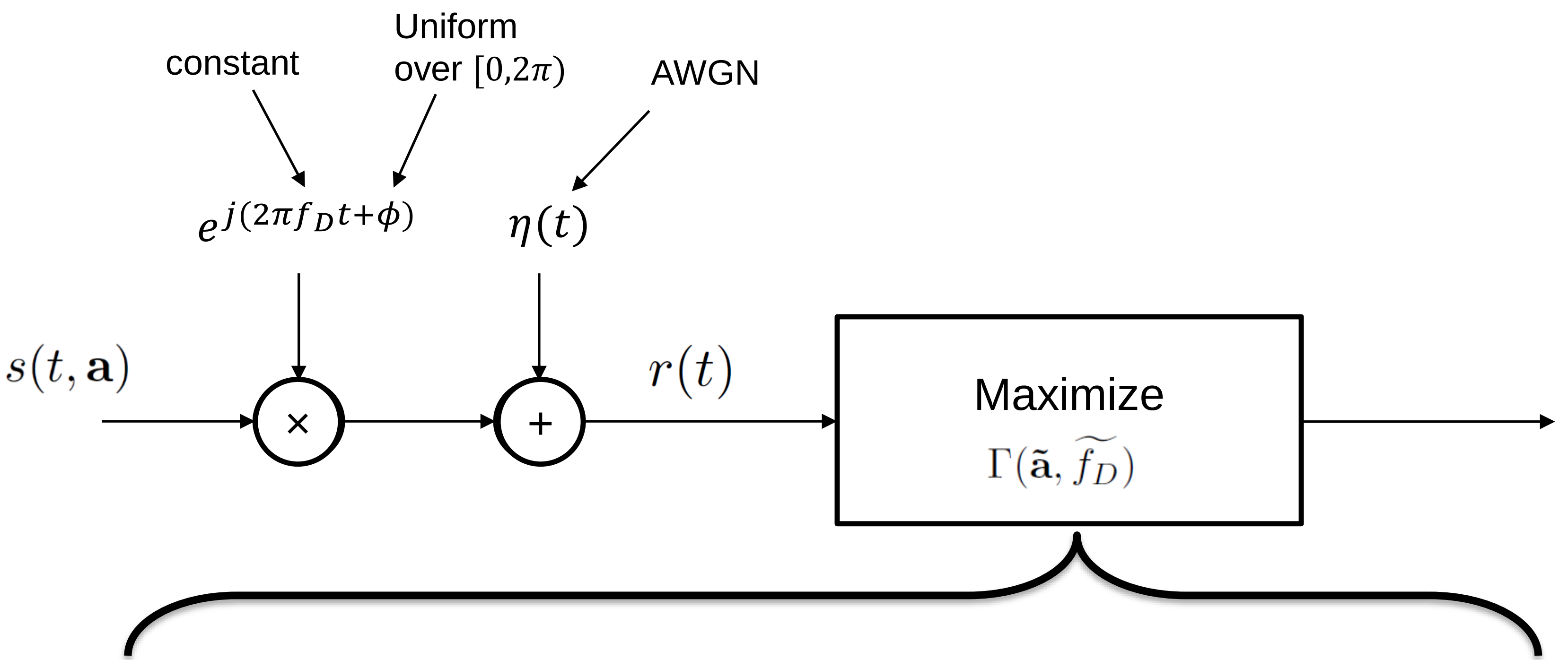

The cost function :

$$\Gamma(\tilde{\mathbf{a}},\widetilde{f_D}) \;=\; \log \mathrm{I}_0\left(\frac{1}{N_0}\left|\int_{T_0} r(t,\mathbf{a})s^*(t,\tilde{\mathbf{a}})e^{-j2\pi\widetilde{f_D}t}dt\right|\right)-\frac{1}{2N_0}\int_{T_0}|s(t,\tilde{\mathbf{a}})|^2dt$$

The generalized likelihood method

- Let
  - $\mathcal{A}$: the set of possible symbol sequences
  - $\mathcal{F}$: the variation interval of f_D (depends on the Doppler profile)

- The generalized likelihood method [1]:

Maximizing $\Gamma(\tilde{\mathbf{a}}, \widetilde{f_D})$ over $\mathcal{A} \times \mathcal{F}$ $\Longleftrightarrow$

$$\max_{\tilde{\mathbf{a}} \in \mathcal{A}} \Gamma(\tilde{\mathbf{a}}, \widehat{f}_D(\tilde{\mathbf{a}}))$$

$$\text{with } \widehat{f}_D(\tilde{\mathbf{a}}) = \arg\max_{\widetilde{f_D} \in \mathcal{F}} \left| \int_{T_0} r(t) s^*(t, \tilde{\mathbf{a}}) e^{-j2\pi \widetilde{f_D} t} dt \right|$$

- Using this criterion, we'll derive two detectors
  - Detector A
  - Detector B

[1] H. L. V. Trees, Detection, estimation and modulation theory. New York: John Wiley & Sons, vol. I, 1968.

Detector A

- Detector A is directly derived from the NSD detector

- Detector A architecture :

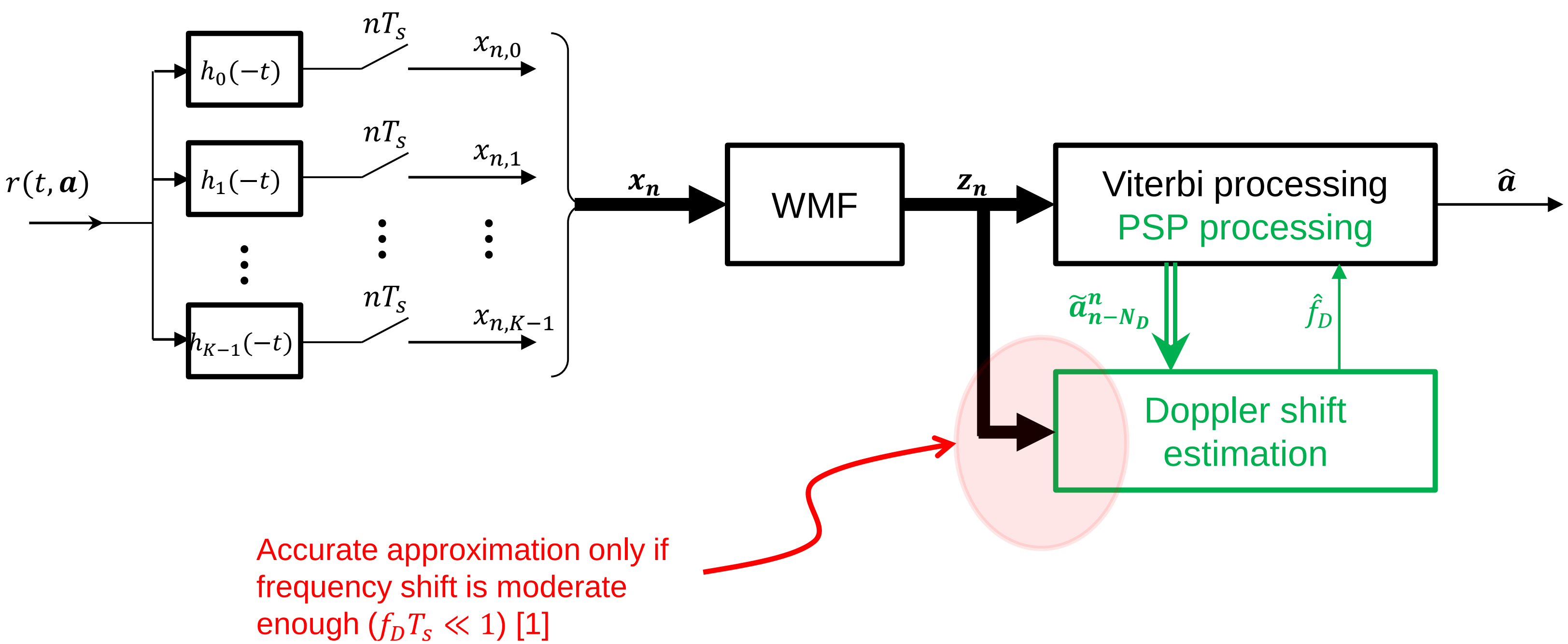

[1] H. Meyr, M. Oerder, and A. Polydoros, “On sampling rate, analog prefiltering, and sufficient statistics for digital receivers,” IEEE Trans. on Commun., vol. 42, no. 12, pp. 3208–3214, 1994.

Detector A

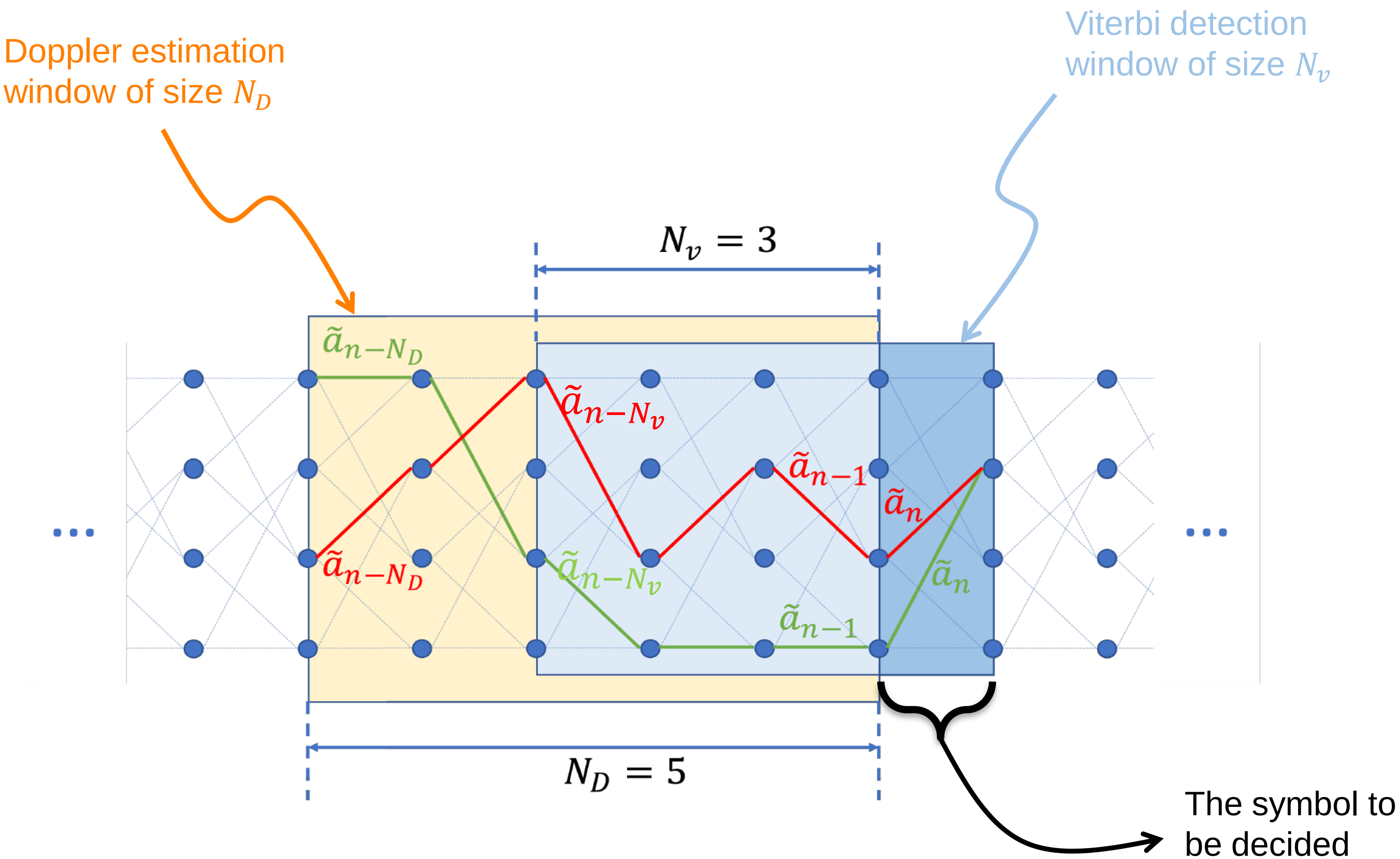
Doppler estimation
window of size N_D
Viterbi detection
window of size N_v
$N_v = 3$
$\tilde{a}_{n-N_D}$
$\tilde{a}_{n-N_v}$
$\tilde{a}_{n-1}$
$\tilde{a}_n$
$\tilde{a}_{n-N_D}$
$\tilde{a}_{n-N_v}$
$\tilde{a}_{n-1}$
$\tilde{a}_n$
$N_D = 5$
The symbol to
be decided

Detector A

- Define a trellis with branch metric :

$$\lambda_n(\tilde{\mathbf{a}}_\mathbf{n}) = \left|\sum_{k=0}^{K_c-1}\sum_{i=0}^{N_v-1} z_{k,n-i}\tilde{y}^*_{k,n-i}e^{-j2\pi(n-i)\widehat{f}_D(\tilde{\mathbf{a}}^n_{n-N_D}))T_s}\right| - \left|\sum_{k=0}^{K_c-1}\sum_{i=1}^{N_v-1} z_{k,n-i}\tilde{y}^*_{k,n-i}e^{-j2\pi(n-i)\widehat{f}_D(\tilde{\mathbf{a}}^n_{n-N_D}))T_s}\right| - \left|\sum_{k=0}^{K_c-1}\tilde{y}_{k,n}\right|^2$$

The branch metric defines the trellis size

Use the same estimation of $\hat{f}_D$ [1]

Instead of $\widehat{f}_D(\tilde{\mathbf{a}}^n_{n-N_D-1}))$

- The estimation of $\hat{f}_D$ is updated through *data-aided* (DA) frequency estimation algorithms using $(\tilde{\mathbf{a}}^n_{n-N_D})$

[1] G. Colavolpe, R. Raheli, and G. Picchi, “Detection of linear modulations in the presence of strong phase and frequency instabilities,” in IEEE Int. Conf. on Communications., vol. 2, 2000, pp. 633–637.

Detector A

- Detector A
  - ✓ Adjustable trellis
  - ✓ Uses few signal samples for detection
  - ⚠ Depends on linear decomposition
  - ⚠ Depends on WMF

➢ Need a more flexible solution !

Detector B

- Detector B focuses on resisting much larger Doppler orders
  - Use the exact expression of CPM signal !

- Detector B architecture :

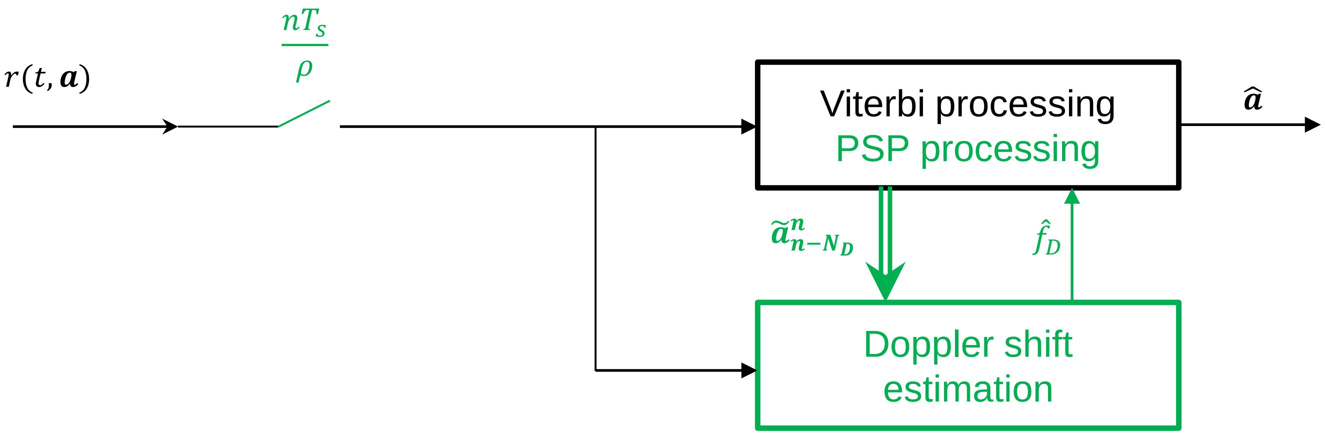

Detector B

- Using the same principles of windowing
  - For Viterbi detection
  - For Doppler estimation

- The branch metrics becomes :

$$\lambda_n(\tilde{\mathbf{a}}) = \left| \int_{(n-N_v)T_s}^{nT_s} v_n(t, \tilde{\mathbf{a}}) s^*(t, \tilde{\mathbf{a}}) dt \right| - \left| \int_{(n-N_v)T_s}^{(n-1)T_s} v_n(t, \mathbf{a}) s^*(t, \tilde{\mathbf{a}}) dt \right|$$

- Where $v_n(t, \tilde{\mathbf{a}}) = r(t, \mathbf{a}) e^{-j2\pi \underbrace{\widehat{f}_D(\tilde{\mathbf{a}}^n_{n-N_D})}t}$

Use the same PSP approach for the estimation

Detector B

- Detector B
  - ✓ Generic architecture
  - ✓ theoretically offers the best Doppler robustness
  - ⚠ More calculation operations due to oversampling

Simulation

Simulation parameters :

Frame length	120
Symbol time (ms)	0.1
Oversampling factor	8
Viterbi detection window length N_v	5
Doppler estimation window length N_D	8
Frequency estimation algorithm	Rife & Boorstyn (ML estimation [1])
Number of FFT points N_{FFT} for frequency estimation	N_{FFT} = 32 (detector A) N_{FFT} = 256 (detector B)

[1] D. C. Rife and R. R. Boorstyn, "Single tone parameter estimation from discrete-time observations," IEEE Trans. Inf. Theory, vol. 20, pp. 591–598, 1974.

Performance comparison between detector A and B

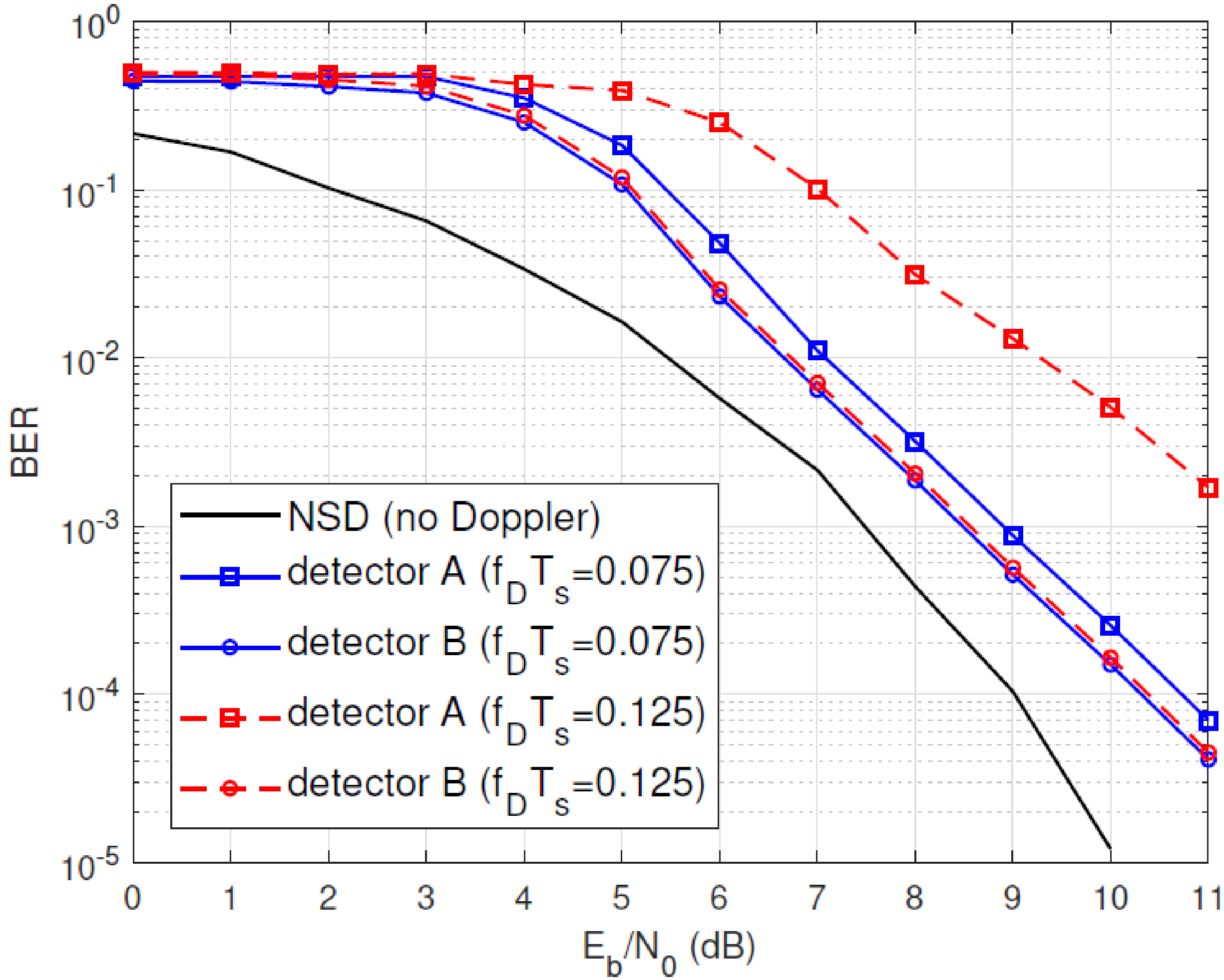

Figure : BER comparison between detectors A ($\rho = 1$, $N_{FFT} = 32$) and B ($\rho = 8$, $N_{FFT} = 256$) for 3RC with $h = 0.75$, $N_v = 5$ and $N_D = 8$

IMT Atlantique
Bretagne-Pays de la Loire
École Mines-Télécom

Performance limitation

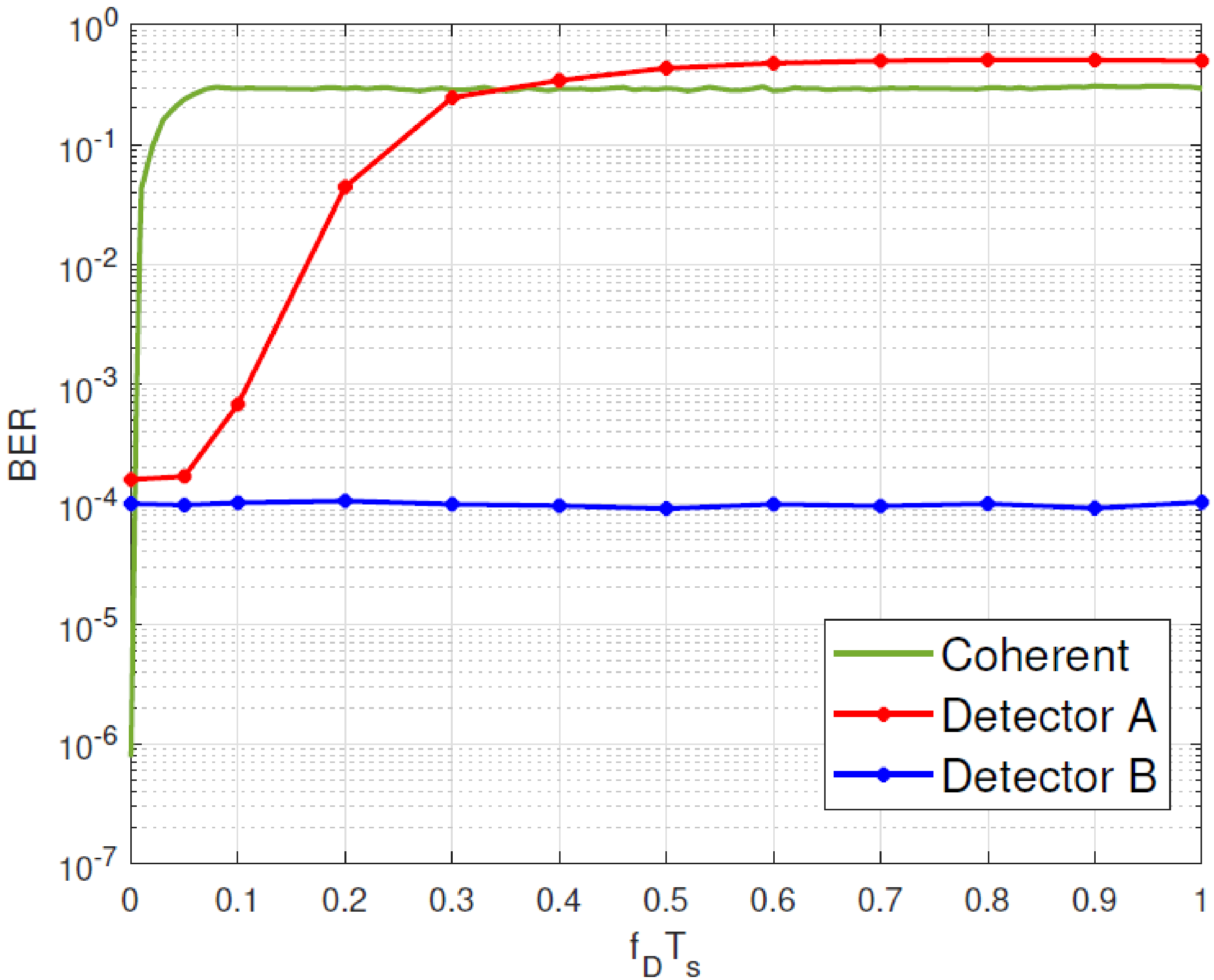

Figure : BER evolution with $f_D T_s$ for detector A and B for the GMSK with N_v = 5 and N_D = 8 at 11 dB

The Doppler rate

- Doppler can vary at a rate of 250 Hz/s !

⚠ If the frame is long enough, the Doppler can not be considered constant

✓ Detector A and B solve this problem by using narrow sliding Doppler estimation window !
  - ➢ Up to 8 symbols of few ms

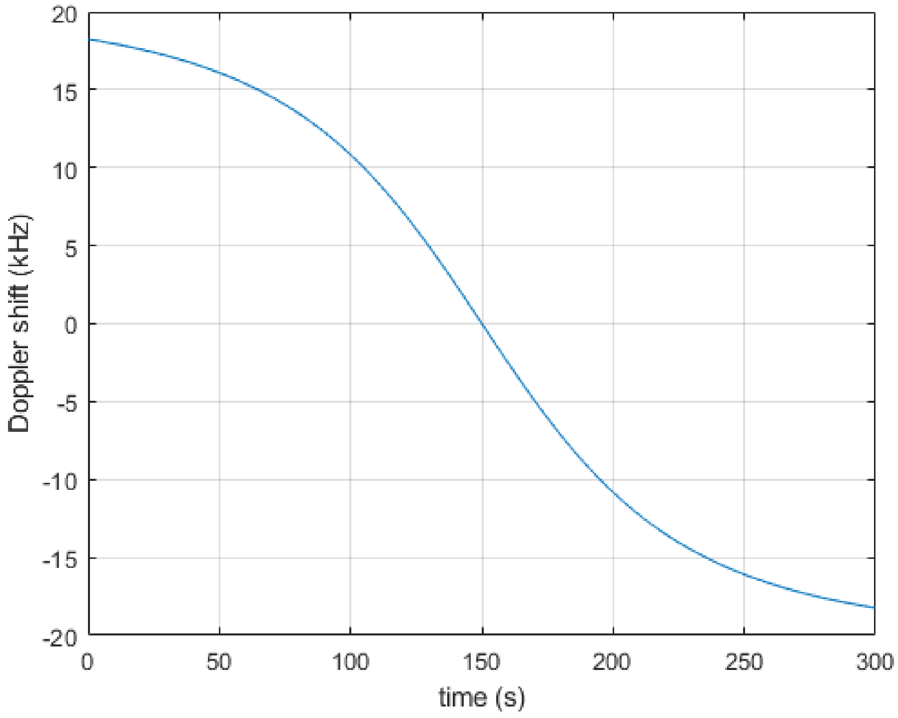

Figure : example of Doppler shift profile received from a LEO satellite when it gets close to the object with 868 MHz carrier at an altitude of 550 km

Performance in presence of Doppler rate

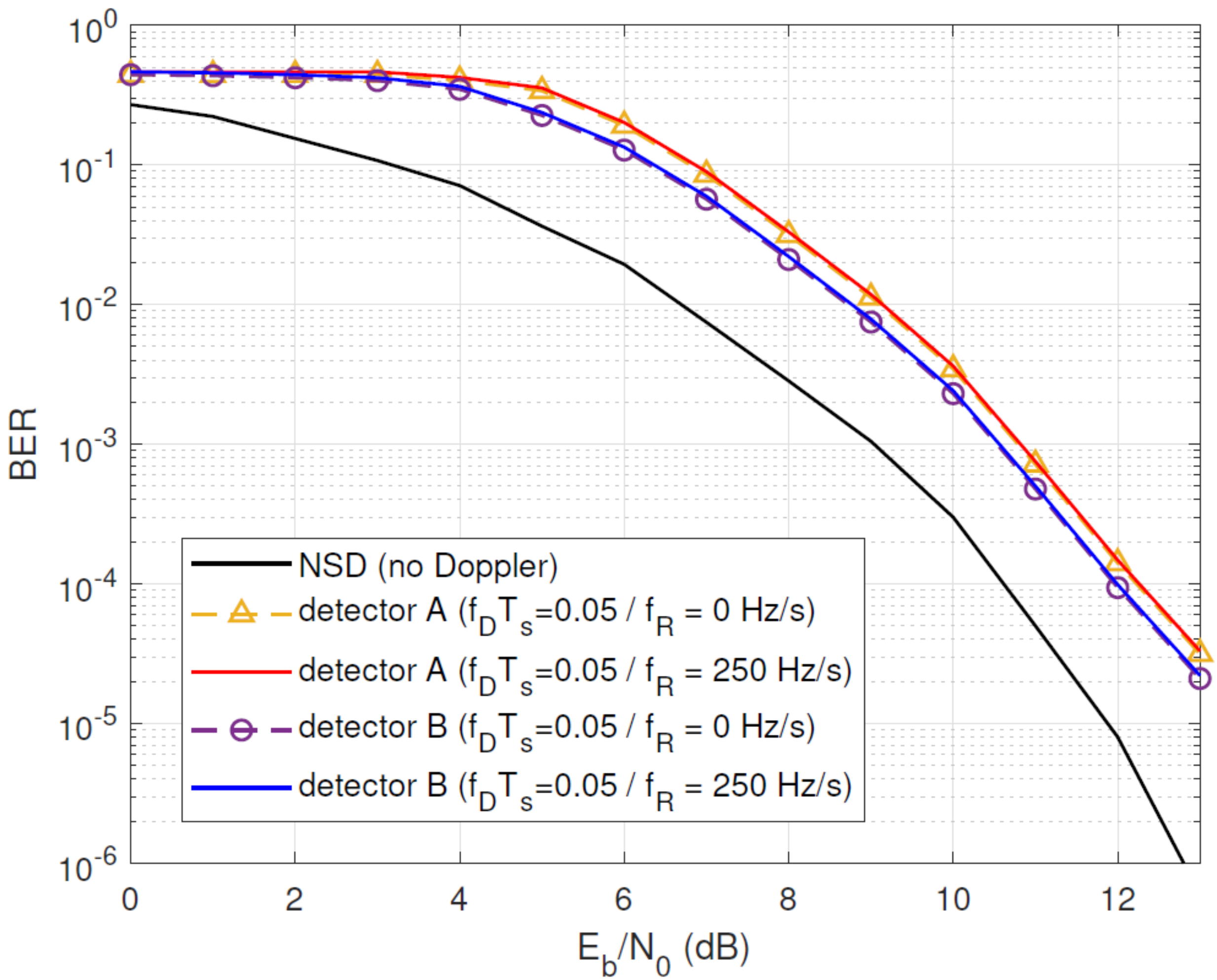

Figure : BER comparison between detector A and B for binary 4RC with $h = \frac{2}{3}$ where $f_D T_s = 0.05$ in presence of Doppler rate $f_R = 250$ Hz/s with $N_v = 5$ and $N_D = 8$

Conclusion

- Detector A and B for the Satellite IoT :
  - ✓ Robustness to Doppler shift
  - ✓ Robustness to Doppler rate
  - ✓ Detection in a blind way

⚠ Still suffer from few drawbacks !

➢ Exploit a different detection approach

OPTIMIZED DELAY DIFFERENTIAL CPM DETECTION

IMT Atlantique
Bretagne-Pays de la Loire
École Mines-Télécom

Transmission model

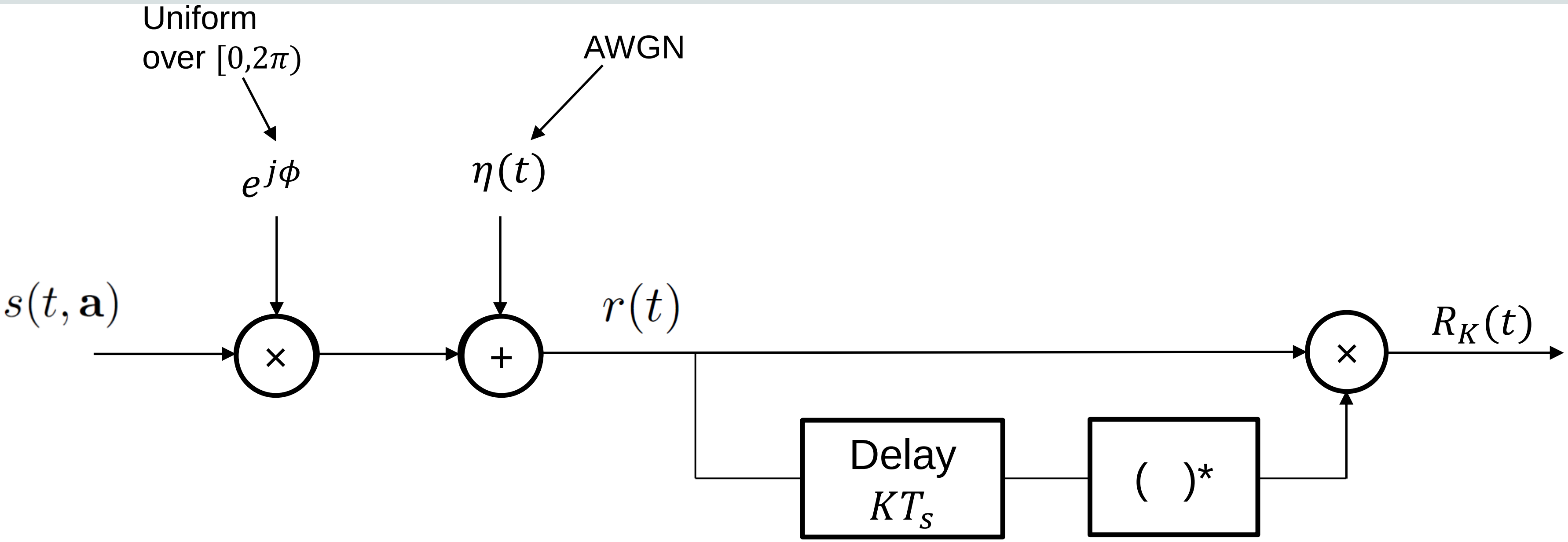

- Differential operation :

$$R_K(t) = \frac{1}{2} r(t) r^*(t - KT_s) = S_K(t,\mathbf{a}) + N_K(t)$$

Noise is assumed to follow a Gaussian distribution [1]

- With

$$S_K(t,\mathbf{a}) = \frac{1}{2} s(t,\mathbf{a}) s^*(t - KT_s,\mathbf{a}) = \frac{E_s}{2T_s} e^{j\Theta_K(t,\mathbf{a})}$$

The new signal phase :

$$\Theta_K(t,\mathbf{a}) = \theta(t,\mathbf{a}) - \theta(t - KT_s,\mathbf{a})$$

[1] D. Makrakis and K. Feher, “Multiple Differential Detection of Con tinuous Phase Modulation signals,” IEEE Transactions on Vehicular Technology, vol. 42, no. 2, pp. 186–196, 1993,

The detection strategy

- ML Detection :
  - maximize the correlation between $R_K(t)$ and all possible realizations of $S_K(t)$

    The cost function : $$\Gamma_N(\tilde{\mathbf{a}}) = \mathrm{Re}\left[\int_0^{NT_s} R_K(t) S_K^{\star}(t, \tilde{\mathbf{a}})dt\right]$$

- Use Viterbi algorithm on the trellis defined by $\Theta_K(t, \mathbf{a})$
- The branch metric : $$\Lambda_n(\tilde{\mathbf{a}}) = \mathrm{Re}\left[\int_{(n-1)T_s}^{nT_s} R_K(t) S_K^{\star}(t, \tilde{\mathbf{a}})dt\right]$$
- The full architecture :

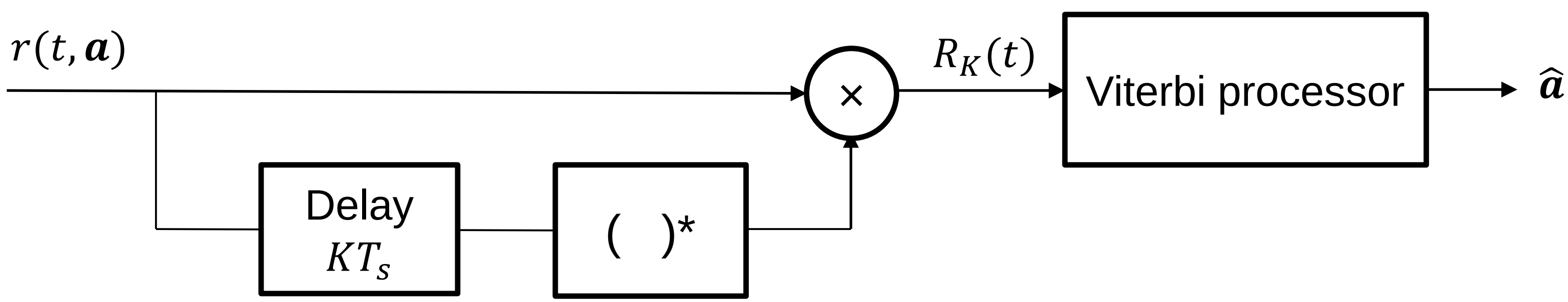

Simulation

Simulation parameters :

Frame length	120
Symbol time (ms)	0.1
Oversampling factor	8
Delay values K	1,2,3,4

Numerical results : influence of the delay

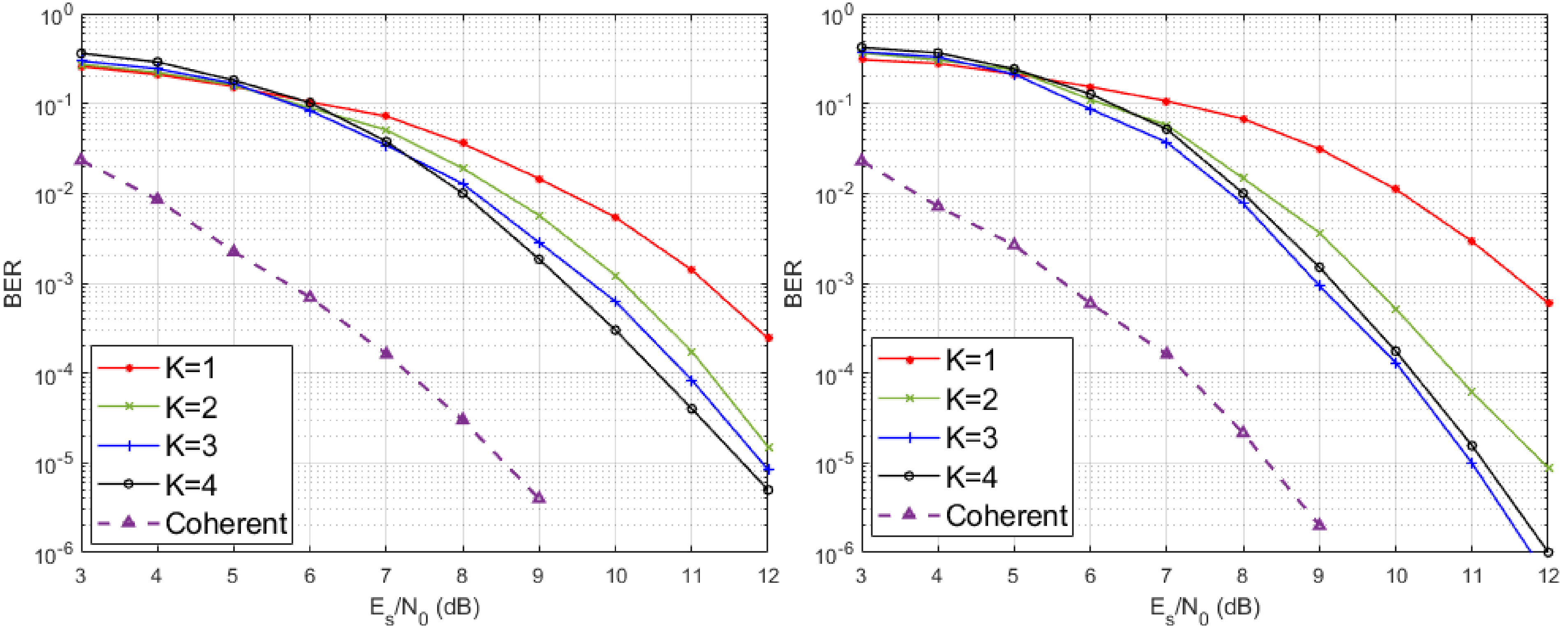

(a) 5RC with h = 0.75

(b) 3REC with h = 0.75

Figure : BER of differential detection for two binary CPM formats for different values of delay K

The differential approach

- Multiple symbol differential detection
  - ✓ Shows performance improvement

⚠ Increasing the delay does not always enhance the performance !

➢ Need to find the optimized delay value !

The delay optimization strategy

- At high SNR :

$$P_e \propto Q\left(\sqrt{\frac{4\varepsilon_b}{N_0^2 + 2A^2 N_0} d_{\min}^2(K)}\right)$$

with $d_{\min}^2(K) = \min_{\substack{\mathbf{a},\tilde{\mathbf{a}} \\ a_0 \neq \tilde{a_0}}} \left(d_K^2(\mathbf{a},\tilde{\mathbf{a}})\right)$

and $d_K^2(\mathbf{a},\tilde{\mathbf{a}}) = \frac{\log_2(M)}{T_s} \int_0^{NT_s} [1 - \cos(\Theta_K(t, \mathbf{e}))] dt$

and $\mathbf{e} = \mathbf{a} - \tilde{\mathbf{a}}$ is the difference symbol sequence

- Finding the minimum Euclidean distance is done by searching over all possible pairs of sequences.
- These pairs are those whose respective paths on a phase tree diverge at time 0 and merge again as soon as possible.
- For each value of the delay K corresponds d_{min}
- K_{opt} is the value that yields the highest d_{min} !

Numerical results : optimized delay values

Freq. pulse length L	Modulation index $h = 1/3$	$h = 1/2$	$h = 3/4$
1	$K = 2$	$K = 2$	$K = 3$
3	$K = 3$	$K = 3$	$K = 3$
5	$K = 4$	$K = 4$	$K = 4$

(a) RC

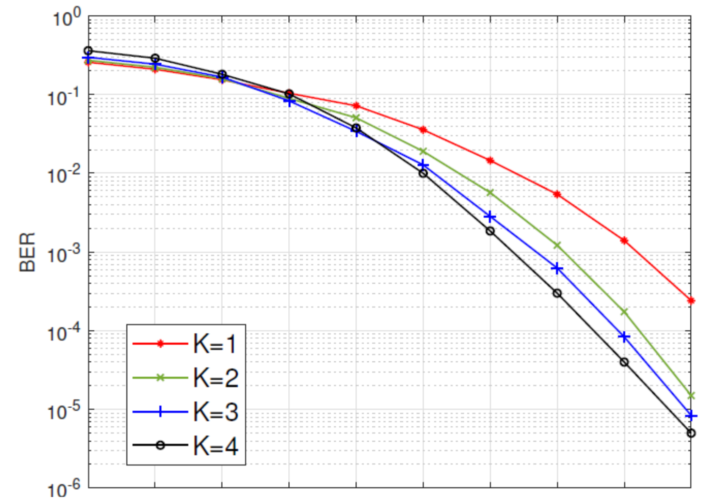

Freq. pulse length L	Modulation index $h = 1/3$	$h = 1/2$	$h = 3/4$
1	$K = 2$	$K = 2$	$K = 4$
3	$K = 4$	$K = 4$	$K = 3$
5	$K = 5$	$K = 5$	$K = 5$

(b) REC

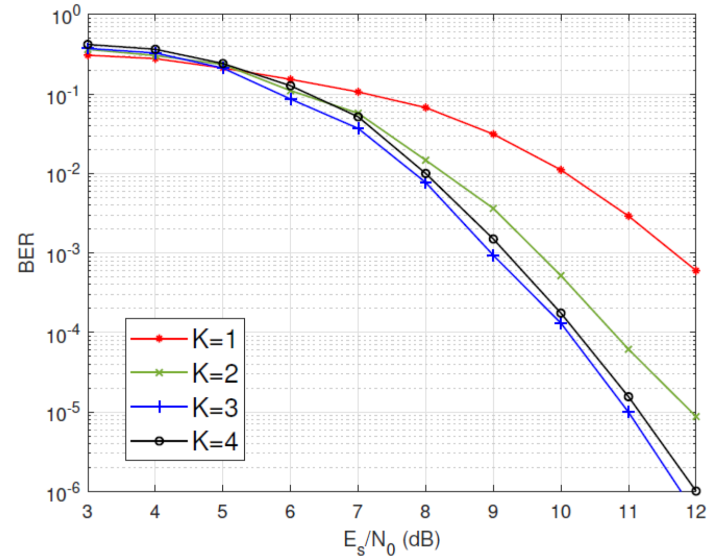

Table : Optimized values of K for some binary CPM schemes

The Doppler problem with differential detector

- In presence of Doppler shift, a constant phase term appears in $R_K(t)$

- The phase term depends on $f_D T_s$:
  - $\Psi = 2\pi K f_D T_s$

- In presence of Doppler rate, the phase term can still be considered constant when having short frames

✓ The optimized delay differential detector showed robustness to this phase term up to a certain order !

Performance in presence of Doppler rate

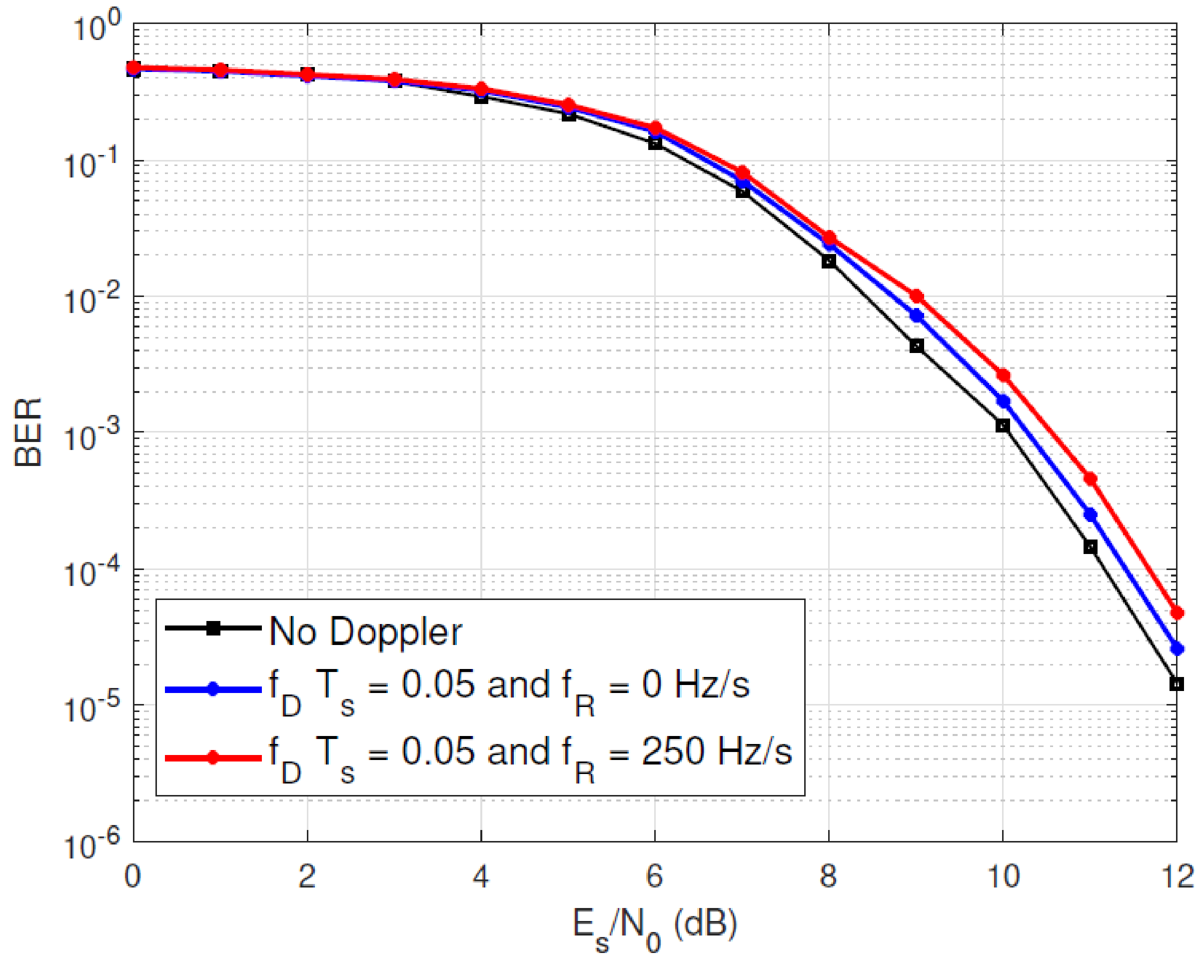

Figure : BER comparison of GMSK with the differential detector with K_{opt} = 3 in presence of no Doppler, Doppler shift only and Doppler shift and rate

Performance in presence of Doppler shift

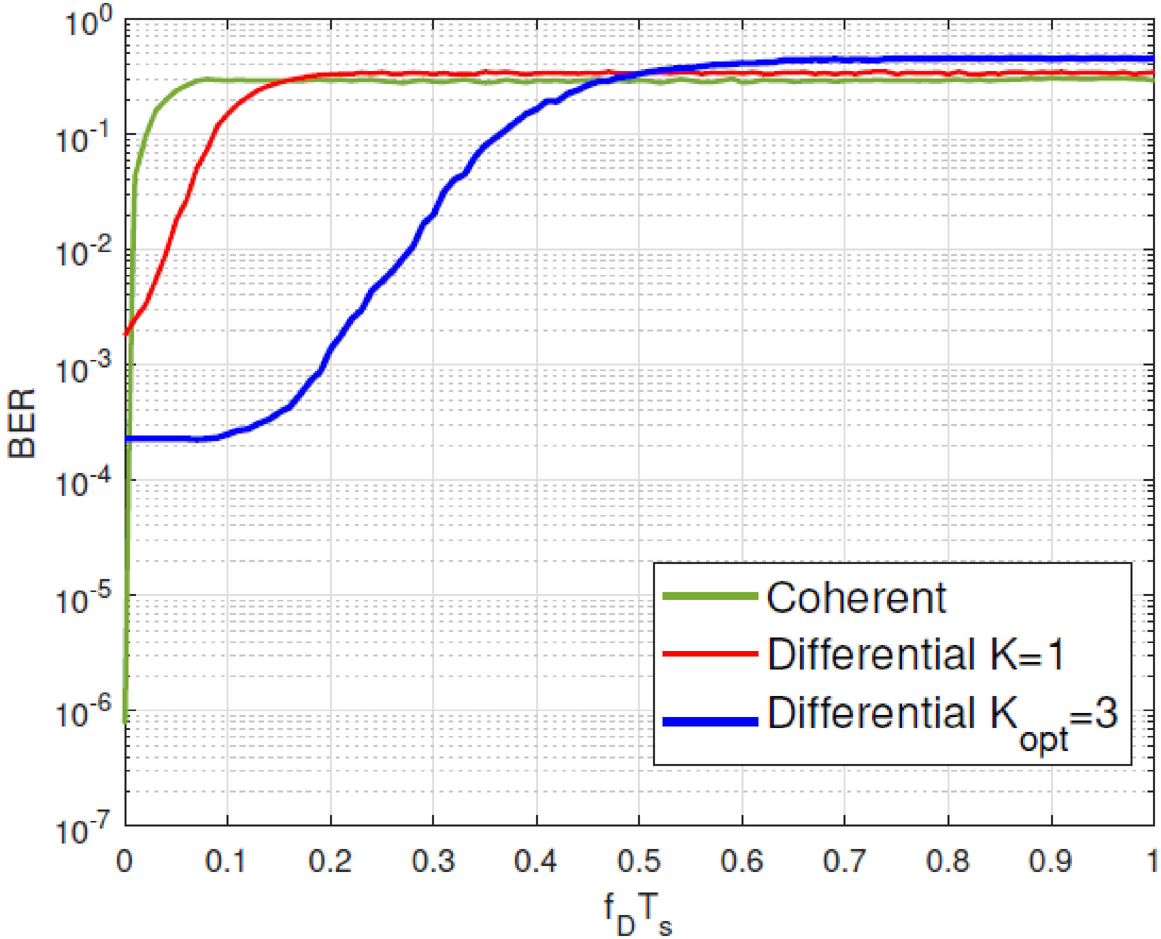

Figure : Comparison of BER evolution with $f_D T_s$ for GMSK for the coherent detector, the differential detector for K = 1 and K_{opt} = 3 at 11 dB of SNR

Performance in presence of Doppler shift

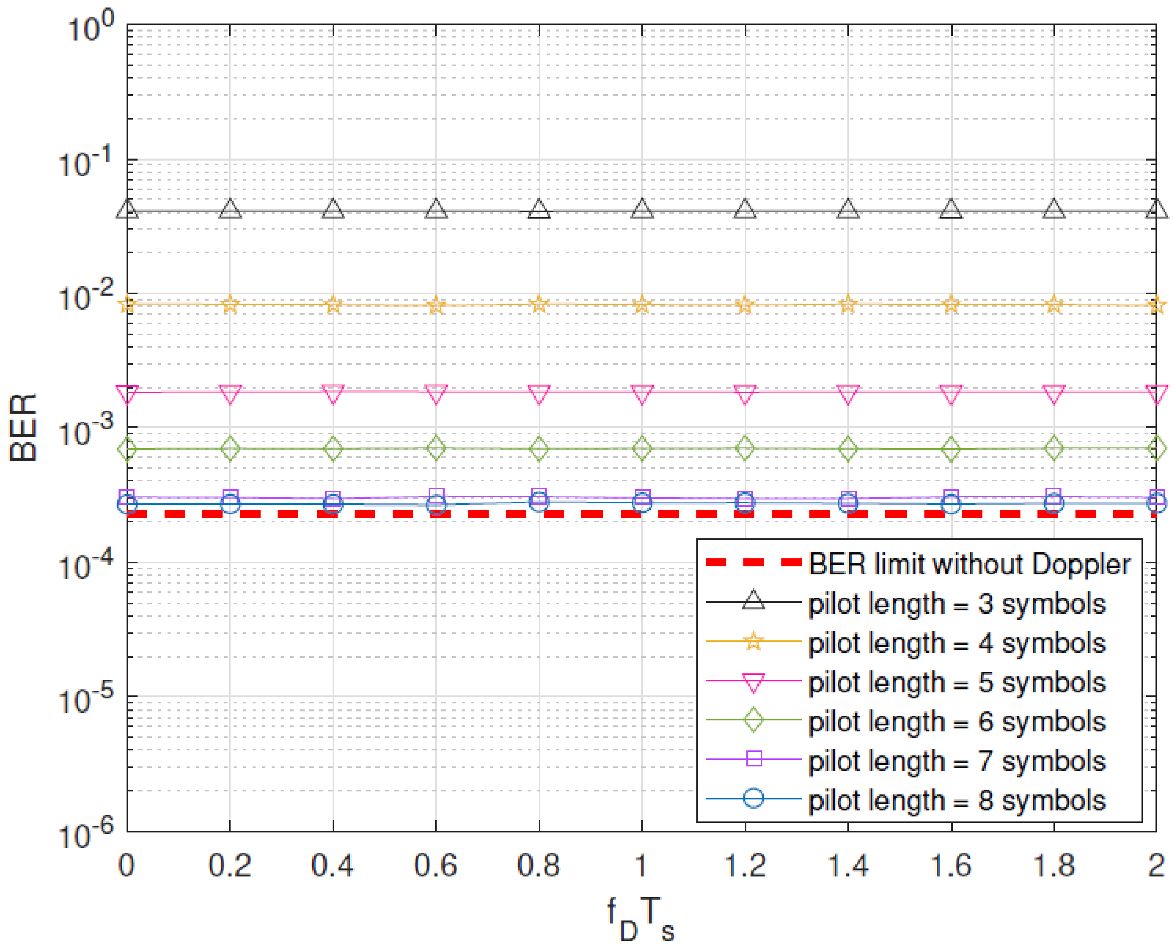

Figure : Comparison of BER evolution with $f_D T_s$ for GMSK for the differential detector with K_{opt} = 3 at 11 dB of SNR using pilot sequence for frequency estimation

Conclusion

- Optimized delay differential detector for the Satellite IoT :
  - ✓ Better performance than the conventional differential detection
  - ✓ Fair robustness to Doppler shift
  - ✓ Robustness to Doppler rate

⚠ Need to use few pilot symbols in very high Doppler order !

COMPARISON BETWEEN DETECTORS

IMT Atlantique
Bretagne-Pays de la Loire
École Mines-Télécom

Complexity comparison

- Algorithm used for frequency estimation : Rife & Boorstyn
  - Involve usage of FFT

- Complexity is assessed through
  - number of trellis states S
  - number of multiplications for metric calculation per trellis section Q_M
  - number of multiplications for Doppler Shift estimation per trellis section Q_D

Detector A: WMF (L_w), Estimation windows (N_v/N_D)
Detector B: CPM memory (L), Estimation windows (N_v/N_D)
Optimized delay differential detector: CPM memory (L), Optimized delay (K_{opt})

Label	Detector A	Detector B	Optimized delay differential detector
S	$M^{N_v+L_w-1}$	M^{N_v+L-2}	$M^{K_{\text{opt}}+L-1}$
Q_M	$(L_w+1)K^2+N_vSM$	$\rho N_v SM$	ρSM
Q_D	$\rho S(N_D+M-1)+MS\frac{N_{\text{FFT}}}{2}\log_2(N_{\text{FFT}})$		none

Table : Comparison of the detectors in terms of complexity figures S, Q_M and Q_D

- With ρ : number of samples per symbol time (ρ=1 for detector A)

Simulation

Simulation parameters :

Frame length	120
Symbol time (ms)	0.1
Oversampling factor	8
Viterbi detection window length N_v	5
Doppler estimation window length N_D	8

BER performance

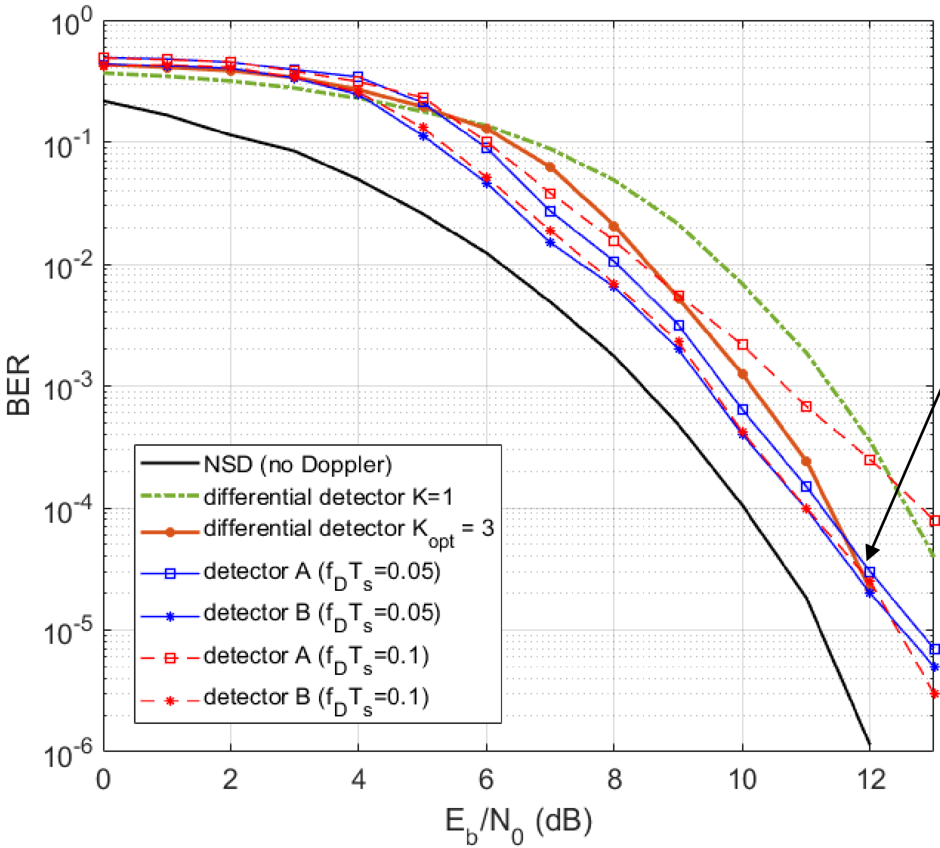

Detectors A and B and differential detector crossing point at $f_D T_s = 0.05$

Label	Detector A (N_{FFT}=32)	Detector B (N_{FFT}=256)	Optimized delay differential detector ($K_{opt} = 3$)
S	64	32	16
Q_M	643	2560	256
Q_D	10816	67840	NA

Table : Numerical values of S, Q_M and Q_D for GMSK

Figure : BER comparison between detectors A (ρ=1, N_{FFT}=32) and B (ρ=8, N_{FFT}=256) with optimized-delay differential detector for GMSK with N_v=5, N_D=8 in presence of Doppler

BER performance

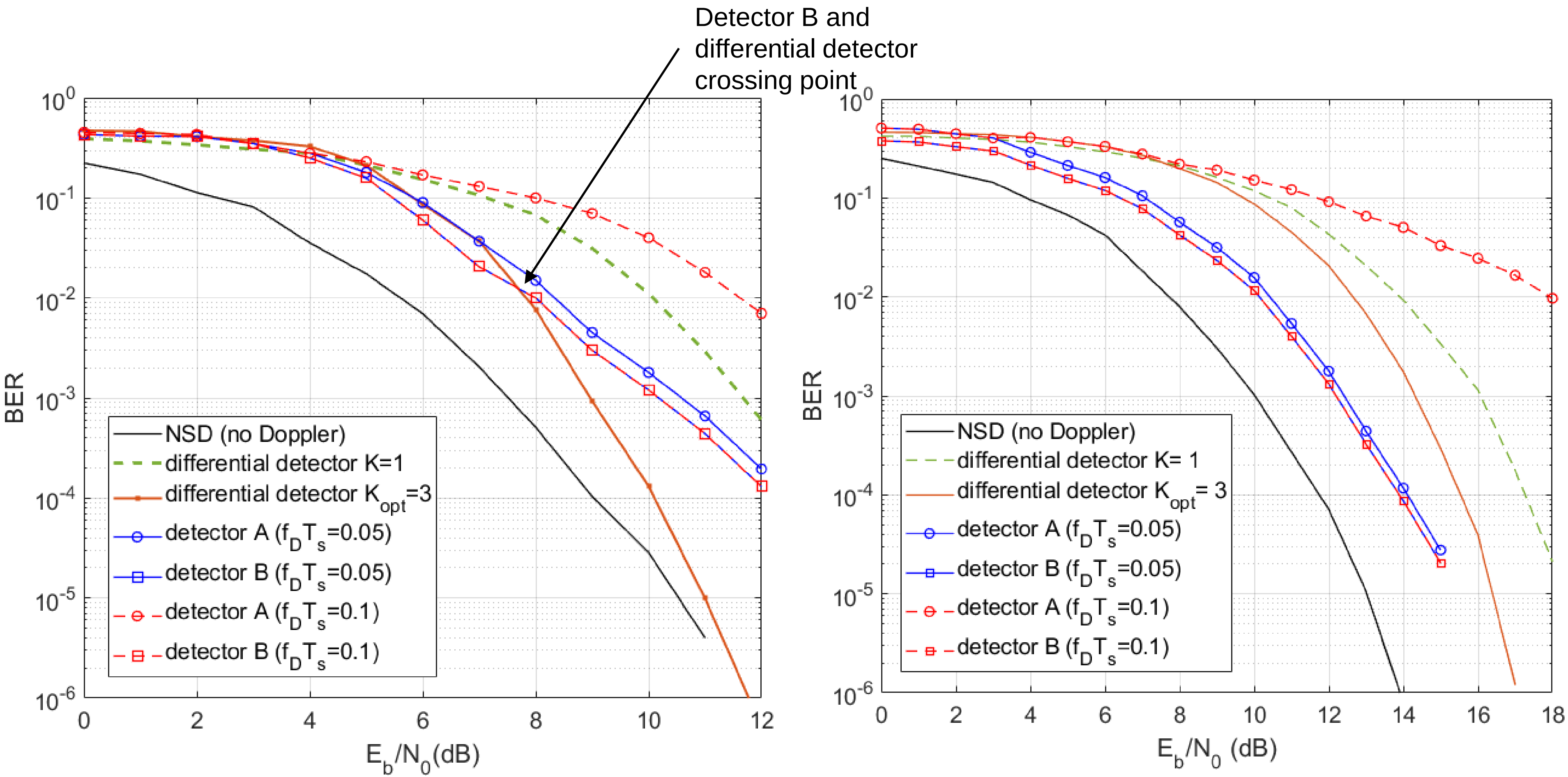

(a) Binary 3REC with h = 0.75 (b) Quaternary 2RC with h = 0.25

Figure : BER comparison between detector B (ρ=8, N_{FFT}=256) and optimized-delay differential detector with N_ν=5, N_D=8 in presence of Doppler for two CPM schemes

Conclusion

- For the Satellite IoT context :

	Error rates without Doppler	Error rates in presence of Doppler	Robustness to Doppler shift	Robustness to Doppler rate	Complexity	Generic architecture
Detector A	★★★	★★	★★	★★★	★★	No
Detector B	★★★	★★	★★★	★★★	★	Yes
Optimized differential detector	★★	★★	★★	★★	★★★	Yes

- More stars means better !

CONCLUSION & PERSPECTIVES

IMT Atlantique
Bretagne-Pays de la Loire
École Mines-Télécom

Conclusion

- For CPM signals :

Detection in presence of Doppler for the Satellite IoT

Adaptation of ML criterion

- Detector A
- Detector B

Preprocessing the received signal

Optimized delay differential detector

✓ Robustness to Doppler shift
✓ Robustness to Doppler rate
✓ Detection in a blind way

- Performances comparison depends on the selected CPM format !

Conclusion

PhD contributions :

- A novel CPM non-coherent detection based on the direct application of the generalized maximum likelihood principle with the insertion of blind Doppler estimation principle of [1] in the proposed algorithm as well as in the CPM non-coherent detection of [2].
- The extension of the usual CPM differential detection algorithm to consider a delay higher than one symbol period (including the description of the phase trellis and the derivation of the equations of the branch and cumulative metrics).
- A method to systematically determine an optimized delay value based on the application of the minimum Euclidean distance criterion between two CPM differential signals.
- The optimized delay values for different CPM formats (modulation index, frequency pulse length, frequency pulse type).

[1] G. Colavolpe, R. Raheli, and G. Picchi, “Detection of linear modulations in the presence of strong phase and frequency instabilities,” in IEEE Int. Conf. on Communications., vol. 2, 2000, pp. 633–637.
[2] G. Colavolpe and R. Raheli, “Noncoherent Sequence Detection of Continuous Phase Modulations,” IEEE Transactions on Communications, vol. 47, no. 9, pp. 1303–1307, 1999.

Perspectives

- Satellite IoT application :
  - Connection of a large number of objects
  - Channel access is mostly random

⚠ High risk of packet collision !!

- Next step :

➡ Investigate a solution for multiuser detection

➡ Focus on synchronization issues

PUBLICATIONS

International Journal

- A. Jerbi, K. Amis, F. Guilloud and T. Benaddi, "Delay Optimization of Conventional Non-Coherent Differential CPM Detection," in IEEE Communications Letters, vol. 27, no. 1, pp. 234-238, Jan. 2023, doi: 10.1109/LCOMM.2022.3220326.

International conference

- A. Jerbi, F. Guilloud, K. Amis and T. Benaddi, "Non-coherent CPM Detection under Gaussian Channel affected with Doppler Shift," 2022 IEEE 33rd Annual International Symposium on Personal, Indoor and Mobile Radio Communications (PIMRC), Kyoto, Japan, 2022, pp. 1338-1343, doi: 10.1109/PIMRC54779.2022.9978066.

National conference

- Anouar Jerbi, Karine Amis, Frédéric Guilloud, Tarik Benaddi. Détection non-cohérente des modulations CPM en présence d’un décalage Doppler. GRETSI’22 : 28ème colloque du Groupement de Recherche en Traitement du Signal et des Images, Sep 2022, Nancy, France, Sep 2022, Nancy, France. hal-03758421f

THANK YOU FOR YOUR ATTENTION !

IMT Atlantique
Bretagne-Pays de la Loire
École Mines-Télécom